A COARSE-MESH TRANSPORT METHOD FOR TIME-DEPENDENT REACTOR PROBLEMS

A Dissertation
Presented to
The Academic Faculty

By

Justin Michael Pounders

In Partial Fulfillment
Of the Requirements for the Degree
Doctor of Philosophy in Nuclear Engineering

Georgia Institute of Technology

May 2010

A COARSE-MESH TRANSPORT METHOD
FOR TIME-DEPENDENT REACTOR PROBLEMS

Approved by:

Dr. Farzad Rahnema, Advisor
Nuclear & Radiological Engineering and Medical Physics Programs
George W. Woodruff School
Georgia Institute of Technology

Dr. Tom Morely
School of Mathematics
Georgia Institute of Technology

Dr. Bojan Petrovic
Nuclear & Radiological Engineering and Medical Physics Programs
George W. Woodruff School
Georgia Institute of Technology

Dr. Benoit Forget
Department of Nuclear Science and Engineering
Massachusetts Institute of Technology

Dr. Dingkang Zhang
Nuclear & Radiological Engineering and Medical Physics Programs
George W. Woodruff School
Georgia Institute of Technology

Dr. Abderrafi Ougouag
Idaho National Laboratory

Date Approved: March 15, 2010

ACKNOWLEDGEMENTS

I would first like to express my gratitude to my advisor, Dr. Farzad Rahnema, for years of valuable instruction and guidance. From my first undergraduate research project, to my Master's thesis and now to my doctoral dissertation, with a few other interesting projects sprinkled along the way, I have learned a tremendous amount.

My sincere appreciation goes to the members of my dissertation reading committee: Dr. Dingkang Zhang, Dr. Bojan Petrovic, Dr. Tom Morely, Dr. Ben Forget and Dr. Abderaffi Ougouag. Thank you all for your insights and service. I am especially grateful to Dr. Dingkang Zhang, for his patience with my almost daily visits to his office as I plumbed the depths of coarse-mesh transport theory.

I would like to express my tremendous appreciation for my wife, Sarah, for her unending love, support and encouragement—finishing this dissertation would have been much harder without her. I am also very grateful for the continuing love and encouragement of my parents, Randy and Lynda Pounders. And to everyone else who has encouraged, counseled and prayed for me over the past several months and years: thank you.

Finally, I gratefully acknowledge the financial support of the Rickover Graduate Fellowship Program sponsored by the Naval Reactors Division of the US Department of Energy, and the mentorship and guidance of Dr. Bernie Bandini and Dr. Ed Tomlinson at Bettis Atomic Power Laboratory.

TABLE OF CONTENTS

LIST OF TABLES

LIST OF FIGURES

SUMMARY

A new solution technique is derived for the time-dependent transport equation. This approach extends the steady-state coarse-mesh transport method that is based on global-local decompositions of large (i.e. full-core) neutron transport problems. The new method is based on polynomial expansions of the space, angle and time variables in a response-based formulation of the transport equation. The local problem (coarse mesh) solutions, which are entirely decoupled from each other, are characterized by space-, angle- and time-dependent response functions. These response functions are, in turn, used to couple an arbitrary sequence of local problems to form the solution of a much larger global problem. In the current work, the local problem (response function) computations are performed using the Monte Carlo method, while the global (coupling) problem is solved deterministically. The spatial coupling is performed by orthogonal polynomial expansions of the partial currents on the local problem surfaces, and similarly, the time-dependent response of the system (i.e. the time-varying flux) is computed by convolving the time-dependent surface partial currents and time-dependent volumetric sources against pre-computed time-dependent response kernels.

CHAPTER 1

INTRODUCTION

The solution of time-dependent neutron transport problems requires significant increases in computational expense relative to steady-state (time-independent) problems. Not only is the problem encumbered with the extra dimension of time, but the inclusion of delayed neutrons—which is required for realistic analyses of reactor transient problems—creates reactor transients that evolve over multiple time scales that can vary up to six orders of magnitude. Yet an accurate model of transient reactor behavior is essential to ensure the safe operation of nuclear power plants.

The desire to produce highly accurate time-dependent reactor solutions is tempered by pressure to solve problems as efficiently as possible. On the one hand, compromising model accuracy necessitates increasing plant operational margins which, in turn, decreases the profitability of the plant. On the other hand, the design, development and deployment of new reactor plants becomes inhibited as the computational expense of the design and analysis tools increases. Although advances in computing power continue to enable increasingly accurate solutions to reactor physics problems, transport-theory-based reactor transient methods remain too expensive for general industrial application. Furthermore, the evolution of reactor designs towards higher compositional heterogeneity and harder (higher energy) neutron spectra have begun pushing advanced reactor concepts away from the regime of traditional reactor physics approximations. Therefore, there is an increasing need to develop sophisticated

reactor physics methodologies that are able to solve complex reactor problems in an efficient manner.

In this dissertation, a novel solution method of the time-dependent neutron transport equation is investigated. This research is an extension of the steady-state coarse mesh transport method (COMET) into the time-dependent problem domain. The response-based coarse mesh transport method has been shown to produce high fidelity solutions to full-core reactor problems using a novel space-angle discretization method that does not rely on spatial homogenization. It has also been shown that the method requires significantly less computational time because of (1) a coarse spatial discretization of the problem and (2) the shifting of some of the computational load to a simplified pre-computational phase.

The goals of this dissertation are the following:

- address the question of how to extend response-based space-angle discretization theory of the coarse mesh transport method to solve time-dependent reactor problems;
- assess how efficiently the time-dependent coarse-mesh transport method performs relative to alternative methods of similar accuracy;
- identify obstacles and challenges that may exist in extending the time-dependent coarse-mesh theory and offer solutions.

To accomplish these goals, a rigorous theoretical framework for approaching the time-dependent response-based method will be developed and approximate equations will be derived that are amenable to numerical solution. To focus the attention of this work on the time variable, only one-dimensional geometries will be considered.

The term "transient" in this dissertation is intended primarily to distinguish the present time-dependent transport problem from steady-state problems. In reactor engineering, the analysis of transient reactor dynamics usually implies the inclusion of thermal hydraulic and other feedback mechanisms that are coupled to the time-dependent transport equation. These multi-physics couplings are beyond the scope of the current research, although a method for including delayed neutrons in the coarse-mesh transport method is presented in Chapter 3. The methods developed in this dissertation are applicable to general time-dependent neutral particle transport, but the specific approach taken is motivated by reactor physics problems.

In the following chapter, a general introduction to time-dependent neutron transport theory is provided followed by a review of common solution methods. This chapter also contains an introduction to the steady-state coarse-mesh transport method that will set the stage for Chapter 3. Chapter 3 derives a rigorous model for the time-dependent coarse-mesh transport theory. The chapter begins with the global-local decomposition of large reactor problems, then presents a derivation of the governing time-dependent response equation that is the fundamental model for the new method. The remainder of the chapter is devoted to developing a numerical approximation of the response equation. The implementation of the approximate response method is discussed in Chapter 4, including both the pre-computational response function generation phase and the algorithm for reconstructing the global problem from the local response function solutions. In Chapter 5, a series of example problems of varying complexity are solved to both verify the theory and implementation of the new method and identify challenges

that remain for future work. Chapter 6 concludes the dissertation and discusses possible extension of the new method to more general reactor transient problems.

CHAPTER 2

BACKGROUND

2.1 Basic Physics and Governing Equations

To predict the power distribution of nuclear fission reactors one must determine the distribution of neutrons in space, energy and time. Because quantum mechanical effects, relativistic adjustments and neutron-neutron interactions can be neglected in reactor physics, the ideal means of determining the neutron distribution is by solving the linearized Boltzmann transport equation. The transport equation for neutrons is an integro-differential equation whose solution provides the neutron density as a continuous function of space ($\mathbf{r}$), energy (E), direction ($\hat{\Omega}$) and time (t). The position vector, $\mathbf{r}$, and the neutron direction, $\hat{\Omega}$, are both three-dimensional vectors in general geometry, (although the direction vector is constrained so that $\hat{\Omega}\cdot\hat{\Omega}=1$) so the solution of the transport equation lies in a continuous seven-dimensional phase space. Because of its complexity, much effort has been exerted in seeking ways to simplify the solution of the transport equation by both mathematical and physical approximation. One of the most common simplifications deals with the energy variable.

Because of complex nuclear interaction resonances, the exact energy dependence of the transport equation is rarely treated explicitly by deterministic solution methods. Instead, the energy domain is often partitioned in a number of contiguous energy sub-intervals or groups. The continuous-energy equation transport equation is then integrated over each energy group independently to provide a set of coupled multigroup equations.

The multigroup transport formulation provides the basis for much of the existing steady-state and transient reactor physics methodologies, and it will likewise be the theoretical starting point for this dissertation. The efficient and accurate collapsing of multigroup parameters is a study unto itself, and there exists a great deal of work on the subject in the literature (Bell and Glasstone 1979; Lewis and W. F. Miller 1993). Within the scope of the present work it will be assumed that all multigroup parameters are given *a priori*.

The general-geometry multigroup time-dependent transport equation can now be expressed as

$$\frac{1}{v_g}\frac{\partial \psi_g(\mathbf{r},\hat{\Omega},t)}{\partial t}+\hat{\Omega}\cdot\nabla\psi_g(\mathbf{r},\hat{\Omega},t)+\sigma_g(\mathbf{r},t)\psi_g(\mathbf{r},\hat{\Omega},t)= \sum_{g'=1}^{G}\int_{4\pi}\left[\sigma_{g',g}(\mathbf{r},\hat{\Omega}\cdot\hat{\Omega}',t)+(4\pi)^{-1}\chi_g(\mathbf{r})\nu\sigma_{fg'}(\mathbf{r},t)\right]\psi_g(\mathbf{r},\hat{\Omega}',t)d\hat{\Omega}'+q_g(\mathbf{r},\hat{\Omega},t) \tag{2.1}$$

where $g=1,2,...,G$ denote the energy groups and

- $\psi_g(\mathbf{r},\hat{\Omega},t)$ is the group g angular neutron flux;
- $\sigma_g(\mathbf{r},\hat{\Omega},t)$ is the group g total cross section;
- $\sigma_{g',g}(\mathbf{r},\hat{\Omega}\cdot\hat{\Omega}',t)$ is the group scattering cross section for neutrons originating in group g' and scattering into group g through an angle $\cos^{-1}\left(\hat{\Omega}\cdot\hat{\Omega}'\right)$;
- $\nu\sigma_{fg}(\mathbf{r},\hat{\Omega},t)$ is the fission neutron production cross section;
- $\chi_g(\mathbf{r})$ is the fission neutron spectrum, normalized so that $\sum_{g'=1}^{G}\chi_{g'}(\mathbf{r})=1$;
- v_g is the group g neutron speed; and
- $q_g(\mathbf{r},\hat{\Omega},t)$ is an external source of neutrons not accounted for by the other terms.

The external source term, $q_g(\mathbf{r},\hat{\Omega},t)$, may represent an arbitrary source of neutrons injected into the reactor (e.g. a start-up source), but the primary source of importance in operational reactor transient analysis is the delayed neutron source.

Delayed neutrons are those that are emitted from the radioactive decay of unstable fission products. Because delayed neutrons are a product of radioactive decay, they appear on a time scale much longer that of neutrons that are emitted directly from the fission event (prompt neutrons). Delayed neutrons typically emerge on the order of seconds or minutes following a fission reaction whereas prompt neutrons are emitted virtually instantaneously. Although delayed neutrons represent a relatively small fraction of the total fission neutron production, their presence is significant enough to substantially influence reactor kinetics, and, in fact, their time delay is what makes reactor control feasible. Unfortunately the vastly different time scales of prompt and delayed neutrons make the solution of the transport equation computationally more challenging by adding a substantial degree of stiffness to the problem.

Rather than explicitly modeling all possible fission fragments and their associated decay chains, it is common to characterize delayed neutrons in terms of a few delayed time groups represented by generic precursors. Each precursor represents a lump density of fission fragments with a single (average) decay constant, and it is assumed that each fission event produces a constant fraction of precursors within each delayed neutron group. Letting $C_i(\mathbf{r},t)$ denote the space and time density of the delayed group i precursor, then

$$\frac{\partial C_i(\mathbf{r},t)}{\partial t} = \beta_i \sum_{g=1}^{G} \nu\sigma_{f,g}\phi_g(\mathbf{r},t) - \lambda_i C_i(\mathbf{r},t) \tag{2.2}$$

where

- β_i is the fraction of all fission neutrons (prompt plus delayed) emitted from the precursor C_i;
- λ_i is the decay constant of precursor C_i; and
- $\phi_g(\mathbf{r},t) = \int_{4\pi} \psi(\mathbf{r},\hat{\Omega},t)d\hat{\Omega}$ is the group g scalar neutron flux.

The delayed neutron emission is introduced into the transport equation as an external source. In the absence of any other external source, this is done by setting $q_g(\mathbf{r},\hat{\Omega},t) = \sum_i \chi_{i,g}\lambda_i C_i$ in Equation (2.1) where the summation extends over all delayed neutron groups. As it is written, the number of neutrons per fission, ν, in Equation (2.1) represents only the prompt neutron emission. It is more common in reactor kinetics, however, to let ν represent the total number of neutrons (prompt plus delayed). In this case, Equation (2.1) takes the form

$$\begin{aligned} &\frac{1}{v_g}\frac{\partial \psi_g(\mathbf{r},\hat{\Omega},t)}{\partial t} + \hat{\Omega}\cdot\nabla\psi_g(\mathbf{r},\hat{\Omega},t) + \sigma_g(\mathbf{r},t)\psi_g(\mathbf{r},\hat{\Omega},t) = \\ &\quad \sum_{g'=1}^{G}\int_{4\pi}\sigma_{g',g}(\mathbf{r},\hat{\Omega}\cdot\hat{\Omega}',t)\psi_g(\mathbf{r},\hat{\Omega}',t)d\hat{\Omega}' + \\ &\quad \frac{(1-\beta)}{4\pi}\chi_{p,g}\sum_{g'=1}^{G}\nu\sigma_{fg'}(\mathbf{r},t)\phi_g(\mathbf{r},t) + \frac{1}{4\pi}\sum_i \chi_{i,g}\lambda_i C_i(\mathbf{r},t) \end{aligned} \tag{2.3}$$

where $\chi_{p,g}$ and $\chi_{i,g}$ are the prompt and delayed neutron spectra, respectively, and $\beta \equiv \sum_i \beta_i$.

The transport and precursor equations have been written here for general geometry for the sake of completeness and to facilitate a comprehensive literature review,

but it will be restricted to one spatial dimension in Chapter X by assuming that the reactor volume is infinite in the two transverse dimensions.

2.2 Time-Dependent Numerical Methods

The solution of Equations (2.1) and (2.2) is dictated by two time scales associated with the prompt and delayed neutron emissions. As a result these equations are stiff differential equations in time, and their solution is dictated by the shortest time scale (the prompt neutron lifetime). This feature, coupled with the inherent complexity of solving the transport equation in energy, direction and space, makes the time-dependent transport problem particularly difficult to solve efficiently.

2.2.1 The Point Reactor Model

Perhaps the simplest treatment of reactor dynamics is the point-reactor model of kinetics, or simply point kinetics (Hetrick 1971; Ash 1979; Bell and Glasstone 1979; Stacey 2001). In this model the time-dependent angular flux is written as the product of an amplitude function, $P(t)$, and a shape function, $\Phi_g(\mathbf{r},\hat{\Omega},t)$:

$$\psi_g(\mathbf{r},\hat{\Omega},t) = P(t)\Phi_g(\mathbf{r},\hat{\Omega},t) \tag{2.4}$$

Although both the amplitude and the space functions are dependent on time, it is assumed that the shape function will be a slowly varying function of time and that the time dependence of the neutron population will primarily be described by the amplitude function. Note that this decomposition is not unique, but it is normally assumed (on physical grounds) that $P(0)=1$ and that $\Phi_g(\mathbf{r},\hat{\Omega},t)$ has a fixed (constant) normalization (Bell and Glasstone 1979).

Based on this decomposition, Equations (2.1) and (2.2) can be written without approximation as (Akcasu, Lellouche et al. 1971; Bell and Glasstone 1979)

$$\frac{dP(t)}{dt} = \frac{\rho(t) - \overline{\beta}(t)}{\Lambda(t)} P(t) + \sum_i \lambda_i c_i(t) \tag{2.5}$$

$$\frac{dc_i(t)}{dt} = \frac{\overline{\beta}_i(t)}{\Lambda(t)} P(t) - \lambda_i c_i(t), \quad i = 1, 2, ... \tag{2.6}$$

where

$$\rho(t) = \frac{1}{F(t)} \sum_{g=1}^{G} \int d\mathbf{r} \int_{4\pi} d\hat{\Omega} \psi_{0g}^{\dagger}(\mathbf{r}, \hat{\Omega}) \left\{ \begin{array}{r} \sum_{g'=1}^{G} \int_{4\pi} \left(\chi_g \Delta \nu \sigma_{f,g'} + \Delta \sigma_{g',g} \right) \psi_{g'}(\mathbf{r}, \hat{\Omega}', t) d\hat{\Omega}' \\ - \Delta \sigma_g \psi_g(\mathbf{r}, \hat{\Omega}, t) \end{array} \right\}$$

$$\overline{\beta}_n(t) = \frac{1}{F(t)} \sum_{g=1}^{G} \int d\mathbf{r} \int_{4\pi} d\hat{\Omega} \psi_{0g}^{\dagger}(\mathbf{r}, \hat{\Omega}) \sum_{g'=1}^{G} \int_{4\pi} d\hat{\Omega}' \chi_{i,g} \beta_i \nu \sigma_{f,g'}(\mathbf{r}, t) \psi_{g'}(\mathbf{r}, \hat{\Omega}', t)$$

$$\overline{\beta}(t) = \sum_i \overline{\beta}_n(t)$$

$$\Lambda(t) = \frac{1}{F(t)} \sum_{g=1}^{G} \int d\mathbf{r} \int_{4\pi} d\hat{\Omega} \frac{1}{v_g} \psi_{0g}^{\dagger}(\mathbf{r}, \hat{\Omega}) \psi_g(\mathbf{r}, \hat{\Omega}, t)$$

$$c_n(t) = \frac{1}{\Lambda(t) F(t)} \sum_{g=1}^{G} \int d\mathbf{r} \int_{4\pi} d\hat{\Omega} \chi_{i,g} C_i(\mathbf{r}, t) \psi_{0g}^{\dagger}(\mathbf{r}, \hat{\Omega})$$

$$F(t) = \sum_{g=1}^{G} \int d\mathbf{r} \int_{4\pi} d\hat{\Omega} \psi_{0g}^{\dagger}(\mathbf{r}, \hat{\Omega}) \sum_{g'=1}^{G} \int_{4\pi} d\hat{\Omega}' \chi_g \nu \sigma_{f,g'}(\mathbf{r}, t) \psi_{g'}(\mathbf{r}, \hat{\Omega}', t)$$

The Δ operator acting on the cross sections in the above definitions takes the difference of the critical cross sections and the perturbed (transient) cross sections. The function $\psi_{0g}^{\dagger}(\mathbf{r}, \hat{\Omega})$ is the critical (time-independent) adjoint flux describing the reactor state immediately before the onset of a transient. Formulating these expressions in terms of the critical adjoint function is necessary to avoid numerical instabilities and to obtain expressions for the reactivity that are relatively insensitive to errors in the flux (Bell and Glasstone 1979).

To this point, there have been no approximations made in developing the point kinetics equations, but Equations (2.5) and (2.6) are purely formal until an appropriate shape function has been determined and the requisite parameters calculated. One could

insert the decomposition of Equation (2.4) into the transport equation and solve for the shape function at each time step, but unless further approximations are made this procedure would be more cumbersome than solving the time-dependent transport equation directly.

For this to be an efficient approach, the shape function should be a slowly varying function of time. The space function is truly time-independent only when the reactor is on an asymptotic period after short-lived transients have died away (i.e. $P(t) \sim e^{\alpha t}$ for some constant α). For this asymptotic case one can reasonably calculate a shape function by solving a form of either the *k*-eigenvalue or α-eigenvalue (depending on the magnitude of the reactivity change) time-independent transport equation (Bell and Glasstone 1979). Alternatively, if the reactor undergoes a small, uniform perturbation from its critical state, then simply making use of the critical shape function often results in reasonable accuracy of the point kinetics equations (Bell and Glasstone 1979). For either of these cases (or any other scenario in which the space function is forced to be truly time-independent) Equations (2.5) and (2.6) are referred to as the point reactor model.

Many scenarios of interest to reactor physicist, however, involve reactor perturbations that are non-uniform in space. For example, control rod movement and xenon/samarium build-up both lead to time-dependent shape functions. The assumption that the shape function does not change in time is therefore invalid in many cases. There are methodologies that explicitly treat the space-time coupling of the time-dependence which will be discussed in the in the next section, but there are also several extensions of

the point reactor model that allow some degree of time variability in the shape factor. Three of these extensions will now be reviewed.

First the *adiabatic approximation* (Ott and Meneley 1969; Akcasu, Lellouche et al. 1971; Bell and Glasstone 1979; Stacey 2001) can be employed when the reactivity changes slowly (e.g. xenon build-up or decay) and one is able to use long time steps relative to the delayed neutron time scales. Under this approximation, the shape function is determined for a given subset of time steps by solving the (static) k-eigenvalue transport equation with combined prompt and delayed neutron emission. This updated shape function is then used to update the point kinetics parameters that are used in the amplitude equation. The disadvantage of this approximation is that no account is made for the time lag of the delayed neutrons, and the shape function is assumed to be completely stationary in time. If the neutron population is growing on a time scale significantly longer than the delayed neutron time scale, however, this approximation is reasonable.

The second common methodology is the *quasistatic approximation* (Ott and Meneley 1969; Hetrick 1971; Bell and Glasstone 1979; Stacey 2001). The quasistatic approximation offers an improvement over the adiabatic method by updating the delayed neutron emission at each time step using the shape functions from previous time steps (rather than the instantaneous shape function.) This improvement takes into consideration the time lag of delayed neutron emission. In some cases the time rate of change of the shape function is also estimated using a first order backward differencing scheme rather than assuming a completely static shape function. This results in the *improved quasistatic approximation* (Ott and Meneley 1969; Goluoglu and Dodds 2001).

Recent work has further extended the quasistatic approximation by replacing the backward difference estimate of the shape function time derivative with a predictor-corrector methodology (Dulla, Mund et al. 2008).

The above extensions to point kinetics all allow shape functions that are non-uniform in time to be considered, and the assumption that the shape function varies slowly in time means that parameter updates can be performed on a much coarser time discretization than the amplitude function which is determined by Equation (2.5). Because calculation of the shape function requires the inversion of the transport operator, significant gains in computational efficiency are obtained by reducing the frequency of the shape function updates. It is also noteworthy that the solution of the amplitude function [Equation (2.5)] is independent of the transport methodology used to solve the static/quasistatic shape function. Previous work has used three-dimensional discrete ordinates (Goluoglu and Dodds 2001), Monte Carlo (Bentley, Demeglio et al. 1997) and diffusion theory (Hetrick 1971; Ash 1979; Stacey 2001).

2.2.2 Modal Expansion and Modal Synthesis Methods

As discussed in the previous section, the space, angle and energy variables are only truly separable from the time variable if the reactor is on an asymptotic period. In this case the amplitude function was set proportional to $e^{\alpha t}$ where α is the asymptotic growth/decay rate of the neutron population (also known as the fundamental mode). A natural extension to this line of thinking is to expand the angular flux in a series of modes (Ash 1979; Bell and Glasstone 1979), i.e. let

$$\psi_g(\mathbf{r},\hat{\Omega},t) = \sum_n T_n(t)\Phi_{n,g}(\mathbf{r},\hat{\Omega}). \tag{2.7}$$

In this *modal expansion*, the $T_n(t)$ can be viewed as time-dependent coefficients of the modes $\Phi_n(\mathbf{r},\hat{\Omega})$. As in point kinetics, this sort of decomposition is not unique until the method of calculating the modes has been determined.

One natural option is to define the modes as the eigenfunctions associated with the period eigenvalues $\{\alpha_n\}$ or multiplication eigenvalues $\{k_m\}$. The period eigenvalue problem is expressed by letting

$$\frac{\partial \psi_g}{\partial t} = \alpha \psi_g,$$
$$\frac{\partial C_i}{\partial t} = \alpha C_i,$$

while the multiplication eigenvalue problem is formulated by dividing the total number of neutrons per fission (prompt plus delayed) by a scaling factor, *k*:

$$\hat{\Omega}\cdot\nabla\psi_g(\mathbf{r},\hat{\Omega}) + \sigma_g(\mathbf{r})\psi_g(\mathbf{r},\hat{\Omega}) = \sum_{g'=1}^{G}\int_{4\pi}\sigma_{g',g}(\mathbf{r},\hat{\Omega}\cdot\hat{\Omega}')\psi_g(\mathbf{r},\hat{\Omega}')d\hat{\Omega}' + \chi_g\sum_{g'=1}^{G}\nu\sigma_{fg'}(\mathbf{r})\phi_g(\mathbf{r})$$

In practice, however, there are mathematical difficulties that prevent the usefulness of this approach due to the complexity of determining the set of eigenvalue-eigenfunction pairs. It has been shown that the set of discrete *k*-eigenvalues may not be complete (Bell and Glasstone 1979), in some cases there are no discrete α-eigenvalues (Kornreich and Parsons 2005) and for both *k*- and α-eigenvalues the discrete set is often augmented by a continuum of eigenvalues (Larsen and Zweifel 1974; Bell and Glasstone 1979). All of these complicating factors make it difficult or impossible to form a complete modal expansion as expressed by Equation (2.7). When the transport problem is simplified via the diffusion or P_1 approximation, however, it has been shown that complete modal

expansions are possible (resulting from the simplified eigen-structure), and these methods have been successfully used to solve reactor kinetics problems (Kaplan 1961; Foulke and Gyftopoulos 1967; Hetrick 1971; Bell and Glasstone 1979; Dulla, Ravetto et al. 2005).

Since a complete modal expansion is typically not feasible in transport theory, a technique called modal synthesis is sometimes employed as an alternative (Kaplan 1966; Ash 1979; Bell and Glasstone 1979). In modal synthesis, the spatial modes are postulated on physical grounds, and the expansion coefficients are determined by a weighted residual method in the space, angle and energy variables. In general, modal synthesis methods have not received much attention in the academic literature because of the often *ad hoc* selection of modes (Bell and Glasstone 1979; Sutton and Aviles 1996), but reasonable results have been obtained in some cases (Kaplan 1966).

2.2.3 Direct Integration Methods

Direct integration methods are in general capable of providing the most accurate solutions of the reactor kinetics equations, but these methods are also the most computationally intensive. Nevertheless, as computing power continues to increase, these methods have been gaining in popularity. Direct methods attempt to solve Equations (2.3) and (2.2) by introducing an approximation for the time derivative of the angular flux that permits one to solve the equations via direct numerical integration. Once the time derivative has been approximated, the transport equation can typically be rewritten as a series of modified static equations.

The most common method of approximating the time derivatives of Equations (2.3) and (2.2) is by differencing techniques. These methods take a partition on the time domain defined by the points $\{t_i\}_{i=0}^{N}$ resulting in N time intervals. It is usually assumed

that the cross sections are constant between two consecutive mesh points. Upon integrating Equation (2.3) over mesh interval n with width $\Delta_n = t_n - t_{n-1}$ we may write

$$\frac{1}{v_g}\frac{\psi_{n,g}(\mathbf{r},\hat{\Omega})-\psi_{n-1,g}(\mathbf{r},\hat{\Omega})}{\Delta_n} = \int_{t_{n-1}}^{t_n}\left\{\mathbf{L}\left[\psi_g(\mathbf{r},\hat{\Omega},t)\right]+\sum_i \chi_{i,g}\lambda_i C_i(\mathbf{r},t')\right\}dt' \qquad (2.8)$$

with $\psi_{n,g}(\mathbf{r},\hat{\Omega}) = \psi_g(\mathbf{r},\hat{\Omega},t_n)$ and the functional $\mathbf{L}\left[\psi_g(r,\hat{\Omega},t)\right]$ defined by

$$\begin{aligned}\mathbf{L}\left[\psi_g(\mathbf{r},\hat{\Omega},t)\right] &= -\hat{\Omega}\cdot\nabla\psi_g(\mathbf{r},\hat{\Omega},t)-\sigma_g(\mathbf{r})\psi_g(\mathbf{r},\hat{\Omega},t)\\ &+\sum_{g'=1}^{G}\int_{4\pi}\sigma_{g',g}(\mathbf{r},\hat{\Omega}\cdot\hat{\Omega}')\psi_g(\mathbf{r},\hat{\Omega}',t')d\hat{\Omega}'+(1-\beta)\chi_{p,g}\sum_{g'=1}^{G}\nu\sigma_{fg'}(\mathbf{r})\phi_g(\mathbf{r},t)\end{aligned}.$$

The θ-method (Sutton and Aviles 1996; Stacey 2001) may now be applied to Equation (2.8), which yields

$$\begin{aligned}\frac{\psi_{n,g}(\mathbf{r},\hat{\Omega})-\psi_{n-1,g}(\mathbf{r},\hat{\Omega})}{v_g\Delta_n} &= \theta\left\{\mathbf{L}\left[\psi_{n,g}(\mathbf{r},\hat{\Omega})\right]+\sum_i\chi_{i,g}\lambda_i C_{n,i}(\mathbf{r})\right\}\\ &+(1-\theta)\left\{\mathbf{L}\left[\psi_{n-1,g}(\mathbf{r},\hat{\Omega})\right]+\sum_i\chi_{i,g}\lambda_i C_{n-1,i}(\mathbf{r})\right\}\end{aligned} \qquad (2.9)$$

with $\theta\in[0,1]$. In diffusion theory and low-order transport theory (e.g. P_1 theory) it is possible to generalize Equation (2.9) (by replacing the group-independent scalar θ with a group-dependent θ_g) and optimize the weighting factors so that the solution of Equation (2.9) is exactly the solution of Equation (2.8) (Stacey 2001). This procedure is computationally intensive, however, because at each time point the complete set of eigenvalues-eigenfunction pairs must be computed for the forward and adjoint diffusion/transport operators (it follows that this approach assumes that the operators have only discrete eigenvalues.) A more common approach is to fix the value of θ (independently of groups) and then define a time partition that delivers reasonable accuracy.

If θ is set to zero then Equation (2.9) becomes a fully (Euler) *explicit* or *forward difference* equation and can be written as

$$\psi_{n,g}(\mathbf{r},\hat{\Omega}) = v_g \Delta_n \left\{ \mathbf{L}\left[\psi_{n-1,g}(\mathbf{r},\hat{\Omega}) \right] + \sum_i \chi_{i,g} \lambda_i C_{n-1,i}(\mathbf{r}) \right\} + \psi_{n-1,g}(\mathbf{r},\hat{\Omega}) \qquad (2.10)$$

The solution of this equation is very efficient computationally since there is no need to invert the transport operator. The resulting solution is first order [$O(\Delta_n)$] accurate in time, but it becomes numerically unstable unless very small time steps are taken (Richtmyer 1957; Lewis and W. F. Miller 1993; Stacey 2001). If a finite difference method is also used on the spatial variable of Equation (2.10), then the stability behavior is a function of both the space and time discretizations (Richtmyer 1957).

On the other hand, if $\theta = 1$ then Equation (2.9) becomes a fully (Euler) *implicit* or *backward difference* equation and can be written as

$$0 = \tilde{\mathbf{L}}\left[\psi_{n,g}(\mathbf{r},\hat{\Omega}) \right] + \sum_i \chi_{i,g} \lambda_i C_{n,i}(\mathbf{r}) + \frac{\psi_{n-1,g}(\mathbf{r},\hat{\Omega})}{v_g \Delta_n} \qquad (2.11)$$

where the transport functional $\mathbf{L}$ has been modified to absorb the term $\left(v_g \Delta_n\right)^{-1} \psi_{n-1,g}(\mathbf{r},\hat{\Omega})$, usually as an adjustment to the total cross section. The solution of this equation is also first order accurate in time, but unlike the explicit difference equation, it is unconditionally stable. The disadvantage of the fully implicit scheme is that the transport operator must be inverted at each time step (this is a fixed source static transport problem with the effective neutron source defined as the right-hand-side of Equation (2.11)). Nevertheless, recent work in time-dependent discrete ordinates methods have used this scheme successfully (Pautz and Birkhofer 2003).

The relative accuracy of the previous two schemes can be improved by setting θ = ½. This is known as the *central* or *diamond difference* scheme. It can be shown that this scheme is second order accurate in time [$O(\Delta_n^2)$] and generally stable, although unphysical oscillations in the solution have been observed when the discretization becomes too coarse (Lewis and W. F. Miller 1993; Stacey 2001). Under the central difference scheme, Equation (2.9) can be written in terms of a center-point solution $\psi_{n-1/2,g}(\mathbf{r},\hat{\Omega})$:

$$0 = \hat{\mathbf{L}}\left[\psi_{n-1/2,g}(\mathbf{r},\hat{\Omega})\right] + \sum_i \chi_{i,g}\lambda_i C_{n-1/2,i}(\mathbf{r}) + \frac{2\psi_{n-1,g}(\mathbf{r},\hat{\Omega})}{v_g \Delta_n} \tag{2.12}$$

The solution at time t_n is then computed by

$$\psi_{n,g}(\mathbf{r},\hat{\Omega}) = 2\psi_{n-1/2,g}(\mathbf{r},\hat{\Omega}) - \psi_{n-1,g}(\mathbf{r},\hat{\Omega}) \tag{2.13}$$

Except for the additional operation represented by Equation (2.13), the central difference scheme is equivalent to the fully implicit scheme in terms of computational expense since both schemes require the inversion of the transport operator at every time step.

The above differencing approximations have been shown for the time-dependent transport equation, but they can be applied to the precursor equation [Equation (2.2)] in an equivalent manner. The two equations can then be explicitly coupled by solving the precursor equation for the unknown term and substituting this into the transport equation (Goluoglu and Dodds 2001; Stacey 2001). Alternatively, it is possible to analytically integrate the i^{th} precursor equation by pre-multiplying by the integrating factor $e^{-\lambda_i(t_n - t)}$, resulting in (Stacey 2001; Turinsky 2001; Downar, Lee et al. 2004)

$$C_{n,i}(\mathbf{r},t_n) = e^{-\lambda_i \Delta_n} C_{n-1,i}(\mathbf{r}) + \beta_i \sum_{g=1}^{G} \int_{t_{n-1}}^{t_n} \nu\sigma_{f,g}\phi_g(\mathbf{r},t')e^{-\lambda_i(t_n - t')}dt' \tag{2.14}$$

If one assumes that the time dependence of the flux has a fixed shape within the time mesh (e.g. linear or quadratic) then the fission term may be integrated analytically and Equation (2.14) may be substituted into the time-dependent transport equation. This approach, coupled with a backward or central difference applied to the scalar flux time derivative, is common in transient nodal diffusion theory (Montagnini, Raffaelli et al. 1996; Turinsky 2001; Downar, Lee et al. 2004).

2.2.4 Nodal Diffusion Theory

Nodal diffusion theory methods do not solve the transport equation, per se, but rather a diffusive approximation to the transport equation. Yet this class of methods constitutes the majority of what is currently used for industrial reactor transient analysis and will therefore be briefly reviewed.

The diffusion description of neutron transport can be obtained by integrating the transport equation over all directions and closing the resulting equation with a form of Fick's Law that relates the scalar flux and the scalar current(Bell and Glasstone 1979; Stamm'ler and Abbate 1983). The diffusion equation can be solved much more efficiently than the transport equation, because the direction of neutron flight no longer needs to be considered, but the solutions will be less accurate in all but the simplest of scenarios.

Nodal diffusion theory further simplifies the reactor problem by homogenizing large sub-regions (nodes) within the reactor. A reasonable degree of accuracy is obtainable by using Generalized Equivalence Theory (GET) (Smith 1986) to approximately conserve node-averaged reaction rates and neutron leakage. (In theory, the use of GET exactly preserves node-averaged reaction rates and leakage, but in practice the homogenized GET parameters are almost always approximated from single-

node lattice calculations.) Once the homogenized parameters have been determined, the diffusion equation is solved using an intra-nodal polynomial expansion of the scalar flux and a finite difference discretization in time (completely analogous to those discussed in Section 2.2.3 for the transport equation).

The widespread popularity of nodal diffusion theory for reactor transient calculations can be attributed to its fast computation times while, unlike the point reactor model, there is no need to assume space-time separability of the flux. In many ways, the methodological approach of nodal diffusion theory is similar to that of the coarse-mesh transport theory that will be discussed in the following section. Namely, there is a pre-computation phase that characterizes the neutronic behavior of large sub-regions of the reactor, followed by a global solution methodology that achieves high efficiency because of the coarse spatial discretization. It will now be shown that the coarse-mesh transport method captures the efficiency of this approach while simultaneous avoiding the two most significant drawbacks of nodal diffusion theory: spatial homogenization and the diffusion approximation.

2.3 Coarse-Mesh Transport Theory

The coarse-mesh transport (COMET) method is a high-order approach for efficiently solving the neutron transport equation over a large spatial domain. To date, the COMET method has been extensively developed for 3D Cartesian and 2D cylindrical steady-state (k-eigenvalue) reactor problems. In this section, the existing steady-state theory will be briefly reviewed to establish certain paradigms that will guide the development of the time-dependent COMET method developed in Chapter 3.

The COMET method is capable of efficiently solving large-scale (full-core) reactor problems with a high order of accuracy. This is accomplished by dividing the

global spatial domain into a set of non-overlapping sub-elements (coarse meshes) that are large relative to the spatial scale (mean free path) of the neutron distribution. For reactor calculations, each coarse mesh typically coincides radially with a fuel assembly. These coarse meshes are coupled by the surface incident and exiting angular fluxes (or, equivalently, the incoming and outgoing partial currents) at mesh. Since the partial currents are not *a priori* known, they must be formulated in terms of pre-computed local response functions.

Response functions characterize the outgoing partial current (the response) from a mesh that results from a given incident partial current. In the original work, based on variational transport theory, the response functions were expressed in terms of surface Green's functions. This approach was later simplified by expanding the incident and exiting partial currents in an orthogonal series. The response functions, in this case, become matrices that relate the coefficients of the incident current expansion to the coefficients of the exiting current expansion. The response functions are determined by solving a series of local transport problems (with linearly independent boundary conditions) within each unique mesh. This approach has been shown to deliver a high order of accuracy without the need of local adjoint solutions that were required with the variational approach. It is this latter approach that serves as the starting point for the time-dependent coarse mesh transport theory.

In general terms, the surface expansion response functions can be formulated by defining a functional that returns the exiting partial current from coarse mesh i [$j^{+}(w_i)$] due to an incident partial current [$j^{-}(w_i)$]:

$$j^{+}(w_i) = \mathbf{R}[j^{-}(w_i)]$$

where w_i is a phase space element on the surface of coarse mesh i. Expressing these partial currents in terms of a local basis set, $\{\varphi_j\}$, results in

$$\sum_p j_p^+ \varphi_p(w_i) = \mathbf{R}\left[\sum_p j_p^+ \varphi_p(w_i)\right].$$

If the basis functions are orthogonal with respect to some inner product, $\langle \varphi_j, \varphi_k \rangle = c_j \delta_{jk}$, then one may use the linearity of the response functional to solve for the expansion coefficients $j_p^{\pm}$:

$$j_p^+ = c_p^{-1} \sum_{p'} j_{p'}^+ \langle \varphi_p, \mathbf{R}[\varphi_{p'}(w_i)] \rangle, \quad p, p' = 1, 2, \ldots .$$

The collection of coefficients, $\langle \varphi_p, \mathbf{R}[\varphi_{p'}(w_i)] \rangle$, for all p and p' constitutes the response function for coarse mesh i. It can be seen that the response function calculations are nothing more than local fixed-source transport problems with boundary conditions $\varphi_{p'}(w_i)$. In 3D Cartesian geometries, choosing the basis functions as products of Legendre polynomials defined along each surface of the mesh has been shown to be very effective. Furthermore, because of the integral nature of the response functions, the Monte Carlo method has been shown to be a very robust and effective tool for their computation.

In summary, the primary advantages of the coarse mesh transport method are

- the global-local decomposition of the spatial domain enables one to efficiently compute transport theory solutions to large problems (i.e. a full reactor core);
- the response functions can be pre-computed for each unique mesh and saved as a permanent library, reducing the final problem to simply iterating on the surface partial currents;

- the use of response functions to generate the local problem solutions precludes the necessity of spatial homogenization;
- the expansions of the interface partial currents in an orthogonal basis set allows one to couple the coarse meshes with a theoretically arbitrary order of accuracy; conversely, if the orthogonal basis is well-conditioned then a high degree of accuracy can be obtained by a relatively low-order expansion;
- the final (global) solution can be made as accurate as the transport method used to evaluate the response functions (e.g. Monte Carlo).

CHAPTER 3

THEORY

The development of time-dependent coarse-mesh will now be addressed. To limit the attention and scope of this work to the time dependence of the transport problem, the spatial domain will be restricted to one dimension. This restriction additionally limits the domain of neutron directions to one dimension (in the polar angle). For notation, we therefore define the phase space as

$$\Re = V \times \Omega$$

with $V = [a,b]$ and $\Omega = [-1,1]$. The time domain will be defined, without loss of generality, as the positive real line:

$$\Im = [0,\infty).$$

The boundary phase space will be decomposed into four elements corresponding to the positive and negative angular half-spaces (Ω^- and Ω^+, respectively) at the two boundary points:

$$\begin{aligned} \partial\Re_a^{\pm} &= \{a\} \times \Omega^{\pm} \\ \partial\Re_b^{\pm} &= \{b\} \times \Omega^{\pm} \end{aligned}.$$

In this simplified context, the general time-dependent transport equation can be written (Bell and Glasstone 1979)

$$\frac{1}{v_g}\frac{\partial \psi_g(x,t)}{\partial t} + \mathbf{H}_g \psi_g(x,t) = \mathbf{F}_g \psi_g(x,t) + q_g(x,t), \quad g = 1,2,...G \tag{3.1}$$

with $(x,t) \in \Re \times \Im$ and the operators $\mathbf{H}_g$ and $\mathbf{F}_g$ defined by

$$\mathbf{H}_g\psi_g(x,t) = \mu\frac{\partial\psi_g(z,\mu,t)}{\partial z} + \sigma_g(z,t)\psi_g(z,\mu,t)$$
$$-\sum_{g'=1}^{G}\int_{-1}^{1}\sigma_{g',g}(z,\mu\mu',t)\psi_g(z,\mu',t)d\mu',.$$
$$\mathbf{F}_g\psi_g(x,t) = \frac{1}{2}\sum_{g'=1}^{G}\int_{-1}^{1}\chi_g\nu\sigma_{fg'}(z,t)\psi_g(z,\mu',t)d\mu'$$

The delayed neutron source has been temporarily lumped into the external source term. To complete the problem definition boundary and initial conditions must be specified. Time-dependent boundary conditions are prescribed in terms of arbitrary boundary operators:

$$\begin{aligned} j_g^-(x_a^-,t) &= \mathbf{B}_a j_g^+(x_a^+,t), \quad x_a^\pm \in \partial\Re_a^\mp \\ j_g^-(x_b^-,t) &= \mathbf{B}_b j_g^+(x_b^+,t), \quad x_b^\pm \in \partial\Re_b^\pm \end{aligned}. \tag{3.2}$$

with the partial currents defined with respect to the surface outward normal directions as

$$\begin{aligned} j_g^+(x,t) &= n(x)\mu\psi_g(x,t), \\ j_g^-(x,t) &= n(x)\mu\psi_g(x,t), \end{aligned} \qquad .$$
$$n(x) = \begin{cases} +1, & x \in \partial\Re_a^- \cup \partial\Re_b^+ \\ -1, & x \in \partial\Re_a^+ \cup \partial\Re_b^- \\ 0, & \text{otherwise} \end{cases}$$

Additionally, a given initial condition is prescribed on the angular flux at time $t = 0$:

$$\psi_g(x,0) = \psi_g^0(x), \quad x \in \Re. \tag{3.3}$$

Equation (3.1) along with conditions (3.2) and (3.3) constitute the *global problem*.

As discussed in Section 2.3, the primary philosophical approach of the steady-state coarse-mesh transport (COMET) method can be summarized in two steps:

1. decompose the global problem into a series of local problems; then
2. couple the local problems using response functions to reconstruct the global problem solution.

The decomposition of the global problem into a sequence of local problems is discussed in next section; the following section presents the response-based framework for the global-local coupling. Both of these sections follow the ideas founded in the previous steady-state work, but are rigorously repeated and extended here with the inclusion of the time variable.

3.1 Global-Local Decomposition

To decompose the global problem into a sequence of local problems, we begin by partitioning the system volume, *V*, into *N* non-overlapping sub-regions (coarse meshes). Let the mesh be defined by the set of points $\{z_n\}_{n=0}^{N}$ such that $z_0 = a$, $z_N = b$ and $z_{n-1} < z_n$ for $1 \le n \le N$. The local problem phase spaces can be defined by

$$\begin{aligned} \Re_n &= [z_{n-1}, z_n] \times \Omega, \quad 1 \le n \le N \\ \partial\Re_n^{\pm} &= \{z_n\} \times \Omega^{\pm}, \qquad 0 \le n \le N \end{aligned}.$$

The local problem is formed by considering Equation (3.1) restricted to one of the $\Re_n$:

$$\frac{1}{v_g}\frac{\partial \psi_{n,g}(x,t)}{\partial t} + \mathbf{H}_g \psi_{n,g}(x,t) = \mathbf{F}_g \psi_{n,g}(x,t) + q_{n,g}(x,t), \quad (x,t) \in \Re_n \times T \,. \tag{3.4}$$

The local problem boundary conditions are formed by replacing the external boundary condition operators of Equation (3.2) with the incoming partial currents from adjacent mesh cells:

$$\begin{aligned} j_{n,g}^{-}(x_{n-1},t) &= j_{n-1,g}^{+}(x_{n-1},t), \quad x_{n-1} \in \partial\Re_{n-1}^{+} \\ j_{n,g}^{-}(x_n,t) &= j_{n+1,g}^{+}(x_n,t), \qquad x_n \in \partial\Re_n^{-} \end{aligned}. \tag{3.5}$$

The initial condition is formed by simply restricting $\psi_{0,g}(x)$ to $\Re_n$:

$$\psi_{n,g}(x,0) = \psi_{n,g}^{0}(x), \quad x \in \Re_n \,. \tag{3.6}$$

Equations (3.4)-(3.6) constitute the *N* local problems resulting from the global problem given in the previous section.

At this point, the formal decomposition of the global problem is exact, and the combination of the local problem solutions, $\psi_{n,g}(x,t)$, is equivalent to the global problem solution. This formulation is useful because it facilitates the decoupling of the local problems. Specifically, it can be seen that each local problem is completely independent of the others except for the time-dependent flow of neutrons through its bounding surfaces. In Section 3.4, the boundary sources will be approximated in a way that permits a complete decoupling of the local problems. First, however, a generalized response equation will be derived to compactly and explicitly represent the local problem solutions in terms of the local boundary and initial conditions.

3.2 The Response Equation

As the name implies, a response equation describes the (neutronic) response of a system given some source term. The driving sources in Equation (3.4) are the initial condition [Equation (3.6)] and any boundary sources [Equation (3.5)]. Instead of applying these sources as conditions on the transport equation, it will be useful in the subsequent analysis to include them as explicit source terms, so that Equation (3.1) has the form

$$\frac{1}{v_g}\frac{\partial \psi_{n,g}(x,t)}{\partial t} + \mathbf{H}_g \psi_{n,g}(x,t) = \mathbf{F}_g \psi_{n,g}(x,t) + q_{n,g}(x,t) + q_{n,g}^{BC}(x,t) + q_{n,g}^{IC}(x)\delta(t) \quad (3.7)$$

where the two additional terms represent the boundary and initial conditions, respectively, and $\delta(t)$ is the Dirac delta function. Note that because the boundary and

initial *sources* are included explicitly in this expression, the boundary and initial *conditions* are replaced by free-surface and zero conditions, respectively.

The incoming partial currents in Equation (3.5) already have the correct definition as a source terms, so the boundary source may be simply defined as

$$q_{n,g}^{BC}(x,t) = \chi_{\partial\Re_{n-1}^{+}}(x) j_{n-1,g}^{+}(x_{n-1},t) + \chi_{\partial\Re_{n}^{-}}(x) j_{n+1,g}^{+}(x_{n},t) \tag{3.8}$$

where $\chi_{\partial\Re_{a}^{\pm}}$ is the characteristic function, satisfying

$$\chi_{\partial\Re_{a/b}^{\pm}}(x) = \begin{cases} 1, & x \in \partial\Re_{a/b}^{\pm} \\ 0, & x \notin \partial\Re_{a/b}^{\pm} \end{cases}.$$

A similar expression for the initial source can be derived by integrating Equation (3.7) over an infinitesimal time interval centered at time $t = 0$:

$$\begin{aligned} \frac{1}{v_g} \lim_{\epsilon \to 0} \left[\psi_{n,g}(x,+\epsilon) - \psi_{n,g}(x,-\epsilon) \right] = q_{n,g}^{IC}(x) + \\ \lim_{\epsilon \to 0} \int_{-\epsilon}^{+\epsilon} \left\{ \left[-\mathbf{H}_g + \mathbf{F}_g \right] \psi_{n,g}(x,t) + q_{n,g}(x,t) + q_{n,g}^{BC}(x,t) \right\} dt \end{aligned}. \tag{3.9}$$

The fact that there are no sources defined for $t < 0$ implies that $\lim_{t \to 0^{-}} \psi_g(x,t) = 0$.

Therefore, Equation (3.9) reduces in the right-hand limit to

$$\frac{1}{v_g} \psi_{n,g}(x,t) = q_{n,g}^{IC}(x). \tag{3.10}$$

Requiring that the original initial condition, Equation (3.3), hold provides a definition for the initial source term:

$$q_{n,g}^{IC}(x) = \frac{1}{v_g} \psi_{n,g}^{0}(x). \tag{3.11}$$

Inserting this definition along with the boundary source term into Equation (3.7) results in

$$\frac{1}{v_g}\frac{\partial \psi_{n,g}(x,t)}{\partial t}+\mathbf{H}_g\psi_{n,g}(x,t)=\mathbf{F}_g\psi_{n,g}(x,t)+q_{n,g}(x,t)+$$
$$\chi_{\partial\Re^+_{n-1}}(x)j^+_{n-1,g}(x_{n-1},t)+\chi_{\partial\Re^-_{n}}(x)j^+_{n+1,g}(x_n,t)+\frac{1}{v_g}\psi^0_{n,g}(x)\delta(t)\,. \qquad (3.12)$$
$$g=1,2,...G$$
$$n=1,2,...N$$

Equation (3.12) accounts for all neutron sources explicitly, rather than using initial and boundary conditions. This formulation makes it possible to write the solution, $\psi_{n,g}(x,t)$, succinctly in terms of Green's functions:

$$\begin{aligned}\psi_{n,g}(x,t)=&\sum_{g'=1}^{G}\int_0^t dt'\int_{\Re_n}dx'\,q_{n,g}(x',t')G_n^{g'\to g}(x'\to x,t'\to t)+\\&+\sum_{g'=1}^{G}\int_0^t dt'\int_{\partial\Re^+_{n-1}}dx'\,j^+_{n-1,g}(x',t')G_n^{g'\to g}(x'\to x,t'\to t)+\\&+\sum_{g'=1}^{G}\int_0^t dt'\int_{\partial\Re^-_{n}}dx'\,j^+_{n+1,g}(x',t')G_n^{g'\to g}(x'\to x,t'\to t)+\\&+\sum_{g'=1}^{G}\int_{\Re_n}dx'\frac{1}{v_g}\psi^0_{n,g}(x')G_n^{g'\to g}(x'\to x,0\to t)+\end{aligned} \qquad (3.13)$$

where the Green's function satisfies

$$\frac{1}{v_g}\frac{\partial G_n^{g'\to g}(x'\to x,t'\to t)}{\partial t}+\mathbf{H}_gG_n^{g'\to g}(x'\to x,t'\to t)=$$
$$\mathbf{F}_gG_n^{g'\to g}(x'\to x,t'\to t)+\delta(x-x')\delta(t-t')\delta_{gg'}\,.$$

An equation for the surface partial currents can be obtained from Equation (3.13) by simply multiplying both sides of the equation by $|\mu|$ and evaluating at the boundary points:

$$
\begin{aligned}
j^{+}_{n,g}(x_{n-1},t) = &\sum_{g'=1}^{G}\int_0^t dt'\int_{\Re_n} dx' q_{n,g}(x',t')\bar{G}_n^{g'\to g}(x'\to x, t'\to t) \\
&+\sum_{g'=1}^{G}\int_0^t dt'\int_{\partial\Re^{+}_{n-1}} dx' j^{+}_{n-1,g}(x',t')\bar{G}_n^{g'\to g}(x'\to x_{n-1}, t'\to t) + \\
&+\sum_{g'=1}^{G}\int_0^t dt'\int_{\partial\Re^{-}_{n}} dx' j^{+}_{n+1,g}(x',t')\bar{G}_n^{g'\to g}(x'\to x_{n-1}, t'\to t) + \\
&+\sum_{g'=1}^{G}\int_{\Re_n} dx' \frac{1}{v_g}\psi^{0}_{n,g}(x')\bar{G}_n^{g'\to g}(x'\to x_{n-1}, 0\to t)
\end{aligned}
\tag{3.14}
$$

$$
\begin{aligned}
j^{+}_{n,g}(x_{n},t) = &\sum_{g'=1}^{G}\int_0^t dt'\int_{\Re_n} dx' q_{n,g}(x',t')\bar{G}_n^{g'\to g}(x'\to x, t'\to t) \\
&+\sum_{g'=1}^{G}\int_0^t dt'\int_{\partial\Re^{+}_{n-1}} dx' j^{+}_{n-1,g}(x',t')\bar{G}_n^{g'\to g}(x'\to x_{n}, t'\to t) + \\
&+\sum_{g'=1}^{G}\int_0^t dt'\int_{\partial\Re^{-}_{n}} dx' j^{+}_{n+1,g}(x',t')\bar{G}_n^{g'\to g}(x'\to x_{n}, t'\to t) + \\
&+\sum_{g'=1}^{G}\int_{\Re_n} dx' \frac{1}{v_g}\psi^{0}_{n,g}(x')\bar{G}_n^{g'\to g}(x'\to x_{n}, 0\to t)
\end{aligned}
\tag{3.15}
$$

where $\bar{G}_n^{g'\to g}(x'\to x_{n-1}, t'\to t) = |\mu| G_n^{g'\to g}(x'\to x_{n-1}, t'\to t)$. Although Equations (3.13)-(3.15) are purely formal at this point (it does not make the solution easier to obtain), these expressions have the desired form of response equations: they provide a formula for the angular neutron flux and surface partial currents in terms of arbitrary neutron sources and a response kernel (the Green's function). Ultimately it will be shown that the response equation for the angular flux [Equation (3.13)] is primarily useful for coupling local transport soltutions in *time*, while the partial current response equations [Equations (3.14)-(3.15)] are primarily useful for coupling local transport solutions in *space*. Also, it will be shown in the next section that there is no need to explicitly compute the Green's functions—they are presently used as a placeholder for an underlying (local) transport calculation. Nevertheless these response equations form the theoretical basis of the

COMET method, and the remainder of this section will be devoted to deriving an approximate solution to these relationships.

3.3 Approximate Solution

Equation (3.13) is a local problem, restricted to the segment (coarse mesh) $\Re_n$ of the larger phase space $\Re = \bigcup_{n=1}^{N} \Re_n$. The problem will also be made local in time by considering only a finite interval of the time domain, say, $\overline{T} = [0,T] \subset \Im$. It will temporarily be assumed that the incoming boundary sources, $j^+_{n-1,g}$ and $j^+_{n+1,g}$, are known. The external source will also be set to zero for notational simplicity, $q_{n,g}(x,t) = 0$. This is not a limiting constraint, however, as the following solution techniques apply equally to the case where $q_{n,g}(x,t) \neq 0$ (an example problem will in fact be shown in Section 5 where the external source is non-zero).

The approximation of Equation (3.13) will be approached in two steps. First, the solution will be approximated over the phase space $\Re_n$ by assuming that the flux may be expressed as a bivariate polynomial in the space-angle variable, *x*. Second, and conceptually similar to the first step, the solution will be expressed as a polynomial in time. These two steps are approached separately because some additional mathematics are required in the time domain that are not required in the space-angle domain.

3.3.1 Phase Space Discretization

We will begin by approximating the boundary and initial source terms as polynomials. If Π_N is the space of polynomials of degree less than or equal to *N*, then we will need a basis that spans $\Pi_Q \times \Pi_R$ over $\Re_n$ for the representation of the initial

source, which is a function of both space and angle everywhere in the coarse mesh, and a basis that spans Π_Q over $\partial\Re_n^{\pm}$ for the boundary sources, which are functions of angle over the coarse mesh boundaries.

As in previous work, we will use the shifted Legendre polynomials, $\left\{\overline{P}_i^I\right\}$, that are orthogonal over an interval, *I*, as the polynomial basis. For the initial source basis functions, we will use

$$P_{qr}^{\Re_n}(x) \equiv \overline{P}_q^{\Omega}(\mu)\overline{P}_r^{V}(z)$$

for $q = 1,2,...,Q$ and $r = 1,2,...,R$. Using the orthogonality of the shifted Legendre polynomials we have

$$\left\langle P_{qr}^{\Re_n}(x), P_{q'r'}^{\Re_n}(x)\right\rangle_{\Re_n} = \frac{2(z_n - z_{n-1})}{(2q+1)(2r+1)}\delta_{qq'}\delta_{rr'}.$$

The projection of the initial source onto the space $\Pi_Q \times \Pi_R$ may therefore be written

$$\psi_{n,g}^{0}(x,t) \approx \psi_{n,g}^{0,(Q,R)}(x,t) = \sum_{q=0}^{Q}\sum_{r=0}^{R}\psi_{n,g}^{0,(q,r)}(t)P_{qr}^{\Re_n}(x)$$

with

$$\psi_{n,g}^{(q,r)}(t) = \frac{(2q-1)(2r-1)}{2(z_n - z_{n-1})}\left\langle P_{qr}^{\Re_n}(x), \psi_{ng}(x,t)\right\rangle_{\Re_n}.$$

[Note that in these expansions, and in subsequent expansions, capital letters will be used to denote the expansion orders (i.e. the degree of the polynomial) and lower-case letters will be used to index the coefficients of the expansions.]

For the boundary sources, we may use the shifted Legendre sets $\left\{\overline{P}_i^{\Omega^+}\right\}$ and $\left\{\overline{P}_i^{\Omega^-}\right\}$ as basis functions. The exiting partial current on the right-hand surface of mesh $\Re_n$, for example may be projected onto Π_Q as

$$j_{n,g}^{+}(x_n^+,t) \approx j_{n,g}^{(Q),+}(x_n^+,t) = \sum_{q=0}^{Q} j_{n,g}^{(q),+}(t;z_n)\overline{P}_q^{\Omega^+}(x_n^+)$$

with

$$j_{n,g}^{(q),+}(t;z_n) = (2q-1)\left\langle \overline{P}_q^{\Omega^+}(x_n^+), j_{n,g}^{+}(x_n^+,t)\right\rangle_{\partial\Re_n^+}.$$

Inserting these approximations into Equation (3.13) leads to

$$\begin{aligned}\psi_{n,g}(x,t) = &\sum_{g'=1}^{G}\sum_{q'=0}^{Q}\int_0^t dt'\, j_{n-1,g}^{(q'),+}(t';z_{n-1})\left[\int_{\partial\Re_{n-1}^+} dx'\,\overline{P}_{q'}^{\Omega^+}(x')G_n^{g'\to g}(x'\to x,t'\to t)\right]+\\ &+\sum_{g'=1}^{G}\sum_{q'=0}^{Q}\int_0^t dt'\, j_{n+1,g}^{(q'),+}(t;z_n)\left[\int_{\partial\Re_n^-} dx'\,\overline{P}_{q'}^{\Omega^+}(x')G_n^{g'\to g}(x'\to x,t'\to t)\right]+\\ &+\sum_{g'=1}^{G}\sum_{q'=0}^{Q}\sum_{r'=0}^{R}\frac{1}{v_g}\psi_{n,g}^{0,(q',r')}\left[\int_{\Re_n} dx'\,P_{q'r'}^{\Re_n}(x')G_n^{g'\to g}(x'\to x,0\to t)\right]\\ &+\varepsilon(x,t)\end{aligned} \qquad (3.16)$$

where $\varepsilon(x,t)$ is the error term incurred by the approximation of the source terms (i.e. the truncation error). Note that the bracketed integrals in each term on the right-hand-side of Equation (3.16) are the transport solutions resulting from source terms taken from the set of basis functions. Because no approximations have been placed on the Green's functions, these local transport solutions are formally exact. The only approximation to this point is in the representation of the aggregate source terms defining the solution $\psi_{n,g}(x,t)$, i.e. the truncation error in the source representation.

Equation (3.16) can be solved by projecting $\psi_{n,g}(x,t)$ onto $\Pi_Q \times \Pi_R$ over $\Re_n$ and requiring that $\varepsilon(x,t)$ be orthogonal to this space. This procedure leads to a set of $(Q+1)(R+1)$ equations for the coefficients of the projection $\psi_{n,g}^{(Q,R)}(x,t)$ in terms of the basis $\left\{P_{qr}^{\Re_n}(x)\right\}_{\substack{q=1,\ldots,Q \\ r=1,\ldots,R}}$:

$$\begin{aligned}\psi_{n,g}^{(q,r)}(t) = &\sum_{g'=1}^{G}\sum_{q'=0}^{Q}\int_0^t dt'\, j_{n-1,g}^{(q'),+}(t')\left\langle P_{qr}^{\Re_n}(x'), \int_{\partial\Re_{n-1}^+} dx'\, \overline{P}_{q'}^{\Omega^+}(x') G_n^{g'\to g}(x'\to x, t'\to t)\right\rangle_{\Re_n} + \\ &+\sum_{g'=1}^{G}\sum_{q'=0}^{Q}\int_0^t dt'\, j_{n+1,g}^{(q'),+}(t)\left\langle P_{qr}^{\Re_n}(x'), \int_{\partial\Re_n^-} dx'\, \overline{P}_{q'}^{\Omega^+}(x') G_n^{g'\to g}(x'\to x, t'\to t)\right\rangle_{\Re_n} + \\ &+\sum_{g'=1}^{G}\sum_{q'=0}^{Q}\sum_{r'=0}^{R}\frac{1}{v_g}\psi_{n,g}^{0,(q',r')}\left\langle P_{qr}^{\Re_n}(x'), \int_{\Re_n} dx'\, P_{q'r'}^{\Re_n}(x') G_n^{g'\to g}(x'\to x, 0\to t)\right\rangle_{\Re_n}\end{aligned} \quad .(3.17)$$

The normed quantities on the right-hand-side of Equation (3.17) are the polynomial moments of the local transport solutions discussed in the previous paragraph. These coefficients form the *response functions* and will hereafter be written more compactly as

$$\begin{aligned}R_{n-1,g',q'}^{n,g,q,r}(t\to t) &= \left\langle P_{qr}^{\Re_n}(x'), \int_{\partial\Re_{n-1}^+} dx'\, \overline{P}_{q'}^{\Omega^+}(x') G_n^{g'\to g}(x'\to x, t'\to t)\right\rangle_{\Re_n} \\ R_{n+1,g',q'}^{n,g,q,r}(t\to t) &= \left\langle P_{qr}^{\Re_n}(x'), \int_{\partial\Re_n^-} dx'\, \overline{P}_{q'}^{\Omega^+}(x') G_n^{g'\to g}(x'\to x, t'\to t)\right\rangle_{\Re_n} \\ R_{g',q',r'}^{n,g,q,r}(t\to t) &= \left\langle P_{qr}^{\Re_n}(x'), \int_{\Re_n} dx'\, P_{q'r'}^{\Re_n}(x') G_n^{g'\to g}(x'\to x, 0\to t)\right\rangle_{\Re_n}\end{aligned} \quad (3.18)$$

so that Equation (3.17) becomes

$$\begin{aligned}\psi_{n,g}^{(q,r)}(t) = &\sum_{g'=1}^{G}\sum_{q'=0}^{Q}\int_0^t dt'\, j_{n-1,g}^{(q'),+}(t';z_{n-1}) R_{n-1,g',q'}^{n,g,q,r}(t'\to t) + \\ &+\sum_{g'=1}^{G}\sum_{q'=0}^{Q}\int_0^t dt'\, j_{n+1,g}^{(q'),+}(t;z_n) R_{n+1,g',q'}^{n,g,q,r}(t'\to t) + \\ &+\sum_{g'=1}^{G}\sum_{q'=0}^{Q}\sum_{r'=0}^{R}\frac{1}{v_g}\psi_{n,g}^{0,(q',r')} R_{n,g',q',r'}^{n,g,q,r}(0\to t)\end{aligned} \quad . \quad (3.19)$$

Equation (3.19) is useful only once the boundary source terms $j_{n\pm1,g}^{(q'),+}(t)$ are known. Because they are not *a priori* known in most cases, they must be incorporated into the solution of the global transport problem. To this end, the surface current response equations (3.14) and (3.15) are approximated in a way that is completely analogous to the angular flux response equation except that the error term is made orthogonal to Π_Q on the surfaces $\partial\Re_n^{\pm}$. The result is

$$\begin{aligned} j_{n,g}^{(q)+}(t;z_{n-1}) = &\sum_{g'=1}^{G}\sum_{q'=0}^{Q}\int_0^t dt'\, j_{n-1,g}^{(q'),+}(t';z_{n-1})\bar{R}_{n-1,g',q'}^{n-1,g,q}(t'\to t) + \\ &+\sum_{g'=1}^{G}\sum_{q'=0}^{Q}\int_0^t dt'\, j_{n+1,g}^{(q'),+}(t';z_n)\bar{R}_{n+1,g',q'}^{n-1,g,q}(t'\to t) + \\ &+\sum_{g'=1}^{G}\sum_{q'=0}^{Q}\sum_{r'=0}^{R}\frac{1}{v_g}\psi_{n,g}^{0,(q',r')}\bar{R}_{n,g',q',r'}^{n-1,g,q}(0\to t) \end{aligned} \tag{3.20}$$

$$\begin{aligned} j_{n,g}^{(q)+}(t;z_n) = &\sum_{g'=1}^{G}\sum_{q'=0}^{Q}\int_0^t dt'\, j_{n-1,g}^{(q'),+}(t';z_{n-1})\bar{R}_{n-1,g',q'}^{n,g,q}(t'\to t) + \\ &+\sum_{g'=1}^{G}\sum_{q'=0}^{Q}\int_0^t dt'\, j_{n+1,g}^{(q'),+}(t';z_n)\bar{R}_{n+1,g',q'}^{n,g,q}(t'\to t) + \\ &+\sum_{g'=1}^{G}\sum_{q'=0}^{Q}\sum_{r'=0}^{R}\frac{1}{v_g}\psi_{n,g}^{0,(q',r')}\bar{R}_{n,g',q',r'}^{n,g,q}(0\to t) \end{aligned} \tag{3.21}$$

with surface response functions defined by

$$\bar{R}^{n-1,g,q}_{n-1,g',q'}(t' \to t) = \left\langle \bar{P}^{\Omega^-}_{q}(x^-_{n-1}), \int_{\partial\Re^+_{n-1}} dx' \bar{P}^{\Omega^+}_{q'}(x') \bar{G}^{g' \to g}_{n}(x' \to x_{n-1}, t' \to t) \right\rangle_{\partial\Re^-_{n-1}}$$

$$\bar{R}^{n-1,g,q}_{n+1,g',q'}(t' \to t) = \left\langle \bar{P}^{\Omega^-}_{q}(x^-_{n-1}), \int_{\partial\Re^-_{n}} dx' \bar{P}^{\Omega^+}_{q'}(x') \bar{G}^{g' \to g}_{n}(x' \to x_{n-1}, t' \to t) \right\rangle_{\partial\Re^-_{n-1}}$$

$$\bar{R}^{n-1,g,q}_{n,g',q',r'}(t' \to t) = \left\langle \bar{P}^{\Omega^-}_{q}(x^-_{n-1}), \int_{\Re_{n}} dx' P^{\Re_n}_{q'r'}(x') \bar{G}^{g' \to g}_{n}(x' \to x_{n-1}, 0 \to t) \right\rangle_{\partial\Re^-_{n-1}}$$

$$\bar{R}^{n,g,q}_{n-1,g',q'}(t' \to t) = \left\langle \bar{P}^{\Omega^+}_{q}(x^+_{n}), \int_{\partial\Re^+_{n-1}} dx' \bar{P}^{\Omega^+}_{q'}(x') \bar{G}^{g' \to g}_{n}(x' \to x_{n}, t' \to t) \right\rangle_{\partial\Re^+_{n}}$$

$$\bar{R}^{n,g,q}_{n+1,g',q'}(t' \to t) = \left\langle \bar{P}^{\Omega^+}_{q}(x^+_{n}), \int_{\partial\Re^-_{n}} dx' \bar{P}^{\Omega^+}_{q'}(x') \bar{G}^{g' \to g}_{n}(x' \to x_{n}, t' \to t) \right\rangle_{\partial\Re^+_{n}}$$

$$\bar{R}^{n,g,q}_{n,g',q',r'}(t' \to t) = \left\langle \bar{P}^{\Omega^+}_{q}(x^+_{n}), \int_{\Re_{n}} dx' P^{\Re_n}_{q'r'}(x') \bar{G}^{g' \to g}_{n}(x' \to x_{n}, 0 \to t) \right\rangle_{\partial\Re^+_{n}}$$

Just as in the angular flux case, these response functions represent the time-dependent polynomial moments of the surface currents that are initiated by source terms that are taken from the basis sets.

Note that in the steady-state case, the response functions do not depend on time. In essence, all responses occur instantaneously with respect to the initiating source, i.e. they are delta functions in time. This leads to the steady-state version of the response moment equations that have been addressed in previous work(Forget 2006; Mosher and Rahnema 2006):

$$\psi^{(q,r)}_{n,g}(t) = \sum_{g'=1}^{G} \sum_{q'=0}^{Q} j^{(q'),+}_{n-1,g}(z_{n-1}) R^{n,g,q,r}_{n-1,g',q'} + \sum_{g'=1}^{G} \sum_{q'=0}^{Q} j^{(q'),+}_{n+1,g}(z_{n}) R^{n,g,q,r}_{n+1,g',q'} \tag{3.22}$$

$$j^{(q)+}_{n,g}(t; z_{n-1}) = \sum_{g'=1}^{G} \sum_{q'=0}^{Q} j^{(q'),+}_{n-1,g}(z_{n-1}) \bar{R}^{n-1,g,q}_{n-1,g',q'}(t' \to t) + \sum_{g'=1}^{G} \sum_{q'=0}^{Q} j^{(q'),+}_{n+1,g}(z_{n}) \bar{R}^{n-1,g,q}_{n+1,g',q'} \tag{3.23}$$

$$j^{(q)+}_{n,g}(t; z_{n}) = \sum_{g'=1}^{G} \sum_{q'=0}^{Q} j^{(q'),+}_{n-1,g}(z_{n-1}) \bar{R}^{n,g,q}_{n-1,g',q'} + \sum_{g'=1}^{G} \sum_{q'=0}^{Q} j^{(q'),+}_{n+1,g}(z_{n}) \bar{R}^{n,g,q}_{n+1,g',q'} \,. \tag{3.24}$$

3.3.2 Time Discretization

In this section, the time-dependence of the response moment equations will be resolved. To start, it will be assumed that the cross sections are independent of time within the interval $\overline{T} = [0, T]$. This simplification leads to a time-invariance of the system responses within $\overline{T}$ that enables the response functions to be written in terms of a single parameter, $\tau \equiv t - t'$, rather than t and t' independently. The parameter τ represents the time delay of responses appearing at time *t* that were initiated by source neutrons at time t'. All response functions of the form $R(t' \to t)$ can therefore be written simply as $R(t - t') = R(\tau)$. Making this substitution in the moments equations [(3.19)-(3.21) in the previous sections] results in

$$\begin{aligned}\psi_{n,g}^{(q,r)}(t) = &\sum_{g'=1}^{G}\sum_{q'=0}^{Q}\int_0^t d\tau\, j_{n-1,g}^{(q'),+}(t-\tau; z_{n-1}) R_{n-1,g',q'}^{n,g,q,r}(\tau) + \\ &+\sum_{g'=1}^{G}\sum_{q'=0}^{Q}\int_0^t d\tau\, j_{n+1,g}^{(q'),+}(t-\tau; z_{n}) R_{n+1,g',q'}^{n,g,q,r}(\tau) + \\ &+\sum_{g'=1}^{G}\sum_{q'=0}^{Q}\sum_{r'=0}^{R}\frac{1}{v_g}\psi_{n,g}^{0,(q',r')} R_{n-1,g',q',r'}^{n,g,q,r}(t)\end{aligned} \tag{3.25}$$

$$\begin{aligned}j_{n,g}^{(q)+}(t; z_{n-1}) = &\sum_{g'=1}^{G}\sum_{q'=0}^{Q}\int_0^t d\tau\, j_{n-1,g}^{(q'),+}(t-\tau; z_{n-1}) \overline{R}_{n-1,g',q'}^{n-1,g,q}(\tau) + \\ &+\sum_{g'=1}^{G}\sum_{q'=0}^{Q}\int_0^t d\tau\, j_{n+1,g}^{(q'),+}(t-\tau; z_{n}) \overline{R}_{n+1,g',q'}^{n-1,g,q}(\tau) + \\ &+\sum_{g'=1}^{G}\sum_{q'=0}^{Q}\sum_{r'=0}^{R}\frac{1}{v_g}\psi_{n,g}^{0,(q',r')} \overline{R}_{n,g',q',r'}^{n-1,g,q}(t)\end{aligned} \tag{3.26}$$

$$\begin{aligned}j_{n,g}^{(q)+}(t; z_{n}) = &\sum_{g'=1}^{G}\sum_{q'=0}^{Q}\int_0^t d\tau\, j_{n-1,g}^{(q'),+}(t-\tau; z_{n-1}) \overline{R}_{n-1,g',q'}^{n,g,q}(\tau) + \\ &+\sum_{g'=1}^{G}\sum_{q'=0}^{Q}\int_0^t d\tau\, j_{n+1,g}^{(q'),+}(t-\tau; z_{n}) \overline{R}_{n+1,g',q'}^{n,g,q}(\tau) + \\ &+\sum_{g'=1}^{G}\sum_{q'=0}^{Q}\sum_{r'=0}^{R}\frac{1}{v_g}\psi_{n,g}^{0,(q',r')} \overline{R}_{n,g',q',r'}^{n,g,q}(t)\end{aligned} \tag{3.27}$$

These three equations all have the same essential form. The first two terms in each equation consist of sums of time-convolution integrals. The response functions in these terms act as convolution kernels that transmit the incoming source information at time $t-t'$ through the local mesh to generate a response at time *t*. The last term in each of these equations represents the straightforward transport of neutrons from the initial source at time $t=0$. The approximate solution of these equations will be derived by considering both of these generic terms in turn.

First, each of the integrals in Equations (3.25)-(3.27) can be represented generally by the expression

$$y(t)=\int_0^t j(t-\tau)R(\tau)d\tau, \quad t\in\overline{T}\,. \tag{3.28}$$

The approximate solution to this equation can be obtained by taking an approach similar to that used in the last section for the space and angle variables. Both the source term, *j*, and the response term, *R*, are continuous functions over $\overline{T}$, so they will be projected onto the polynomial space Π_S on $\overline{T}$ using the shifted Legendre polynomials, $\left\{\overline{P}_s^{\overline{T}}\right\}_{s=0,1,\ldots S}$ as basis functions:

$$j(t-\tau)\approx j^{(S)}(t-\tau)=\sum_{s=0}^{S} j^{(s)}\overline{P}_s^{\overline{T}}(t-\tau)$$

$$R(\tau)\approx R^{(S)}(\tau)=\sum_{s=0}^{S} R^{(s)}\overline{P}_s^{\overline{T}}(\tau)$$

with

$$j^{(s)}=\frac{2s+1}{T}\left\langle \overline{P}_s^{\overline{T}}(t), j(t)\right\rangle_{\overline{T}}$$

$$R^{(s)}=\frac{2s+1}{T}\left\langle \overline{P}_s^{\overline{T}}(t), R(t)\right\rangle_{\overline{T}}$$

for $s = 0,1,...,S$. Inserting these approximations into Equation (3.28) yields

$$y(t) \approx \sum_{s=0}^{S}\sum_{s=0}^{S} j^{(s)} R^{(s')} \int_0^t \overline{P}_s^{\overline{T}}(t-\tau)\overline{P}_{s'}^{\overline{T}}(\tau)d\tau \,. \tag{3.29}$$

To resolve the integral in Equation (3.29), the shifted Legendre polynomials will be expressed in terms of the monomial basis $\left\{t^s\right\}_{s=1}^{S}$. Denoting the expansion coefficients of the monomial expansion with overbars, Equation (3.29) becomes

$$y(t) \approx \sum_{s=0}^{S}\sum_{s=0}^{S} \overline{j}^{(s)} \overline{R}^{(s')} \int_0^t (t-\tau)^s \tau^{s'} d\tau \,. \tag{3.30}$$

Repeated integration by parts then yields

$$y(t) \approx \sum_{s=0}^{S}\sum_{s=0}^{S} \overline{j}^{(s)} \overline{R}^{(s')} \frac{s!(s')!}{(s+s'+1)!} t^{s+s'+1} \,. \tag{3.31}$$

This polynomial approximation of the integral equation (3.30) has been briefly studied in the literature (Chang and Wang 1985; Chang, Yang et al. 1987). In (Chang, Yang et al. 1987) Equation (3.31) was written in matrix-vector notation as

$$y(t) \approx \overline{\mathbf{j}}^T \left[\overline{\mathbf{R}}_0 \; \overline{\mathbf{R}}_1\right] \begin{bmatrix} \boldsymbol{\theta}(t) \\ t^{s+1}\boldsymbol{\theta}(t) \end{bmatrix} \tag{3.32}$$

with

$$\overline{\mathbf{j}} = \begin{bmatrix} \overline{j}^{(0)} & \overline{j}^{(1)} & \dots & \overline{j}^{(S)} \end{bmatrix}^T$$

$$\boldsymbol{\theta}(t) = \begin{bmatrix} 1 & t & \dots & t^S \end{bmatrix}^T$$

$$\overline{\mathbf{R}}_0 = \begin{bmatrix} 0 & r_{0,0} & r_{0,1} & \dots & r_{0,s-1} \\ & 0 & r_{1,0} & \dots & r_{1,s-2} \\ & & \ddots & & \vdots \\ & & & 0 & r_{s-1,0} \\ & & & & 0 \end{bmatrix}_{(s+1)\times(s+1)}$$

$$\overline{\mathbf{R}}_1 = \begin{bmatrix} r_{0,s} & 0 & & & \\ r_{1,s-1} & r_{1,s} & 0 & & \\ \vdots & \vdots & \ddots & & \\ r_{s-1,1} & r_{s-1,2} & \dots & r_{s-1,s} & 0 \\ r_{s,0} & r_{s,1} & \dots & r_{s,s-1} & r_{s,s} \end{bmatrix}_{(s+1)\times(s+1)}$$

where $r_{0,j} = \frac{1}{j+1}\overline{R}^{(j)}$ and $r_{i,j} = \frac{i}{i+j+1} r_{i-1,j}$ for $i > 0$. This form of the equation was then solved by forming a matrix, $\mathbf{P}_m$, that approximates the higher order monomials (degree greater than s) in terms of lower order polynomials:

$$y(t) \approx \overline{\mathbf{j}}^T \left[\overline{\mathbf{R}}_0 + \overline{\mathbf{R}}_1 \mathbf{P}_m \right] \boldsymbol{\theta}(t) . \tag{3.33}$$

In the current work this procedure produced significant error unless very high order expansions were used. An alternative technique has been developed, therefore, that is believed to be better conditioned than Equation (3.33).

Instead of approximating the higher order terms with lower order terms in the monomial basis (which is known to be ill-conditioned), Equation (3.33) is simply translated back to the Legendre basis and truncated. Because the Legendre coefficients generally decay very rapidly, the truncation error should be acceptable for reasonable values of *S*. Letting $\mathbf{B}_s$ be the transformation matrix from the monomial basis to the shifted Legendre basis, i.e.

$$\begin{bmatrix} j^{(0)} \\ j^{(1)} \\ \vdots \\ j^{(s)} \end{bmatrix} = \mathbf{B}_s \begin{bmatrix} \overline{j}^{(0)} \\ \overline{j}^{(1)} \\ \vdots \\ \overline{j}^{(s)} \end{bmatrix},$$

then Equation (3.32) can be rewritten as

$$\begin{aligned} y(t) &\approx \mathbf{j}^T \mathbf{B}_s^{-T} \left[\overline{\mathbf{R}}_0 \ \overline{\mathbf{R}}_1 \right] \mathbf{B}_{2s+1}^T \mathbf{P}_{2s+1}(t) \\ &\approx \mathbf{j}^T \mathbf{B}_s^{-T} \overline{\mathbf{R}}_0 \mathbf{B}_s^T \mathbf{P}_s(t) \end{aligned} \tag{3.34}$$

where terms corresponding to Legendre orders greater than s have been truncated in the second expression. Finally, projecting $y(t)$ onto Π_s over $\overline{T}$ and requiring that the error term be orthogonal to this space results in

$$\mathbf{y} = \mathbf{B}_s \overline{\mathbf{R}}_0 \mathbf{B}_s^{-1} \mathbf{j} \tag{3.35}$$

where the column vector $\mathbf{y}$ contains the $(s+1)$ expansion coefficients of $y(t)$. It is important to note that once the response coefficients are known, the matrix $\mathbf{B}_s \overline{\mathbf{R}}_0 \mathbf{B}_s^{-1}$ only needs to be computed once. This matrix, which relates the time-coefficients of the response, **y**, to the time-coefficients of the source, **j**, can then be used in all subsequent computations without modification.

Having now derived an approximation of the integral terms of the time-response equations [(3.25)-(3.27)], all that remains is to approximate the response of the initial source which has the following general form:

$$y(t) = \psi R(t) .$$

As in the integral terms, the response function is approximated by a polynomial in time. In this case, however, the source is truly a delta function in time, so there is no need to convolve the response against the source. The result may be written

$$\mathbf{y} = \psi \mathbf{R} \tag{3.36}$$

where

$$\begin{aligned} \left[\mathbf{y}\right]_i &= y^{(i)} = \frac{2i+1}{T}\left\langle \overline{P}_i^{\overline{T}}(t), y(t)\right\rangle_{\overline{T}}, \\ \left[\mathbf{R}\right]_i &= R^{(i)} = \frac{2i+1}{T}\left\langle \overline{P}_i^{\overline{T}}(t), R(t)\right\rangle_{\overline{T}}, \quad i = 0,1,...s \end{aligned}.$$

Applying these approximations to the original equations [(3.25)-(3.27)] yields the final form of the approximate response equations:

$$\begin{aligned} \boldsymbol{\psi}_{n,g}^{(q,r)} = &\sum_{g'=1}^{G}\sum_{q'=0}^{Q} \mathbf{R}_{n-1,g',q'}^{n,g,q,r} \mathbf{j}_{n-1,g}^{(q'),+}(z_{n-1}) + \\ &+ \sum_{g'=1}^{G}\sum_{q'=0}^{Q} \mathbf{R}_{n+1,g',q'}^{n,g,q,r} \mathbf{j}_{n+1,g}^{(q'),+}(z_n) + \\ &+ \sum_{g'=1}^{G}\sum_{q'=0}^{Q}\sum_{r'=0}^{R} \frac{1}{\nu_g} \psi_{n,g}^{0,(q',r')} \mathbf{R}_{n,g',q',r'}^{n,g,q,r} \end{aligned}, \tag{3.37}$$

$$\begin{aligned} \mathbf{j}_{n,g}^{(q)+}(z_{n-1}) = &\sum_{g'=1}^{G}\sum_{q'=0}^{Q} \overline{\mathbf{R}}_{n-1,g',q'}^{n-1,g,q} \mathbf{j}_{n-1,g}^{(q'),+}(z_{n-1}) + \\ &+ \sum_{g'=1}^{G}\sum_{q'=0}^{Q} \overline{\mathbf{R}}_{n+1,g',q'}^{n-1,g,q} \mathbf{j}_{n+1,g}^{(q'),+}(z_n) + \\ &+ \sum_{g'=1}^{G}\sum_{q'=0}^{Q}\sum_{r'=0}^{R} \frac{1}{\nu_g} \psi_{n,g}^{0,(q',r')} \overline{\mathbf{R}}_{n,g',q',r'}^{n-1,g,q} \end{aligned}, \tag{3.38}$$

$$\begin{aligned} \mathbf{j}_{n,g}^{(q)+}(z_n) = &\sum_{g'=1}^{G}\sum_{q'=0}^{Q} \overline{\mathbf{R}}_{n-1,g',q'}^{n,g,q} \mathbf{j}_{n-1,g}^{(q'),+}(z_{n-1}) + \\ &+ \sum_{g'=1}^{G}\sum_{q'=0}^{Q} \overline{\mathbf{R}}_{n+1,g',q'}^{n,g,q} \mathbf{j}_{n+1,g}^{(q'),+}(z_n) + \\ &+ \sum_{g'=1}^{G}\sum_{q'=0}^{Q}\sum_{r'=0}^{R} \frac{1}{\nu_g} \psi_{n,g}^{0,(q',r')} \overline{\mathbf{R}}_{n,g',q',r'}^{n,g,q} \end{aligned}. \tag{3.39}$$

Several important features of these equations follow:

- Equation (3.37) can be thought of as the solution equation proper—it is this equation that provides the distribution of neutrons in space and time in the coarse mesh over $\Re_n$; this is in contrast to…
- Equations (3.38) and (3.39)—these equations provide the spatial coupling between coarse meshes via the interface partial currents;
- All of the response coefficients can be computed without any *a priori* knowledge of the global solution (this is a key point for the next chapter);
- Any functional of the flux (e.g. fission rate distribution) can be expressed by an equation similar to those listed above by applying that functional to both sides of the original response equation [Equation (3.13)] and following through the approximation procedure outlined in this section.

3.4 Delayed Neutrons

Delayed neurons represent an additional source term in the neutron transport equation. The strength of the source (i.e. the density of the delayed neutron precursors), however, is a functional of the scalar flux so that a coupled set of equations must be solved. In this section, a solution technique for the delayed neutron precursor equation will be presented. For each delayed group, the precursor equation has the following form:

$$\frac{\partial C(z,t)}{\partial t} = \beta F(z,t) - \lambda C(z,t), \quad z \in V_n, t \in \Im$$

where $F(z,t) = \sum_{g=1}^{G} \nu\sigma_{f,g}(z,t) \int_{-1}^{1} \psi_g(z,\mu,t) d\mu$. The spatial dependence of this equation will be represented using shifted Legendre polynomials as was similarly done for the angular flux. This leads to the following set of moments equations:

$$\frac{\partial C^{(q)}(t)}{\partial t} = \beta F^{(q)}(t) - \lambda C^{(q)}(t), \quad q = 1, 2, ..., Q \tag{3.40}$$

where

$$C^{(q)}(t) = \frac{2q+1}{z_n - z_{n-1}} \left\langle \overline{P}_q^{V_n}(z), C(z,t) \right\rangle_{V_n}$$
$$F^{(q)}(t) = \frac{2q+1}{z_n - z_{n-1}} \left\langle \overline{P}_q^{V_n}(z), F(z,t) \right\rangle_{V_n}.$$

Integrating equation (3.40) from 0 to t yields

$$C^{(q)}(t) = C^{(q)}(0) + \beta \int_0^t F^{(q)}(t')dt' - \lambda \int_0^t C^{(q)}(t')dt'.$$

Now proceeding as usual by expanding the time-dependence in shifted Legendre polynomials over the finite time interval $\overline{T}$ and additionally making use of the identity

$$\int_0^t \overline{P}_s^{\overline{T}}(t')dt' = \frac{1}{2s+1}\left[\overline{P}_{s+1}^{\overline{T}}(t') - \overline{P}_{s-1}^{\overline{T}}(t') \right]_{t'=0}^{t},$$

leads to

$$\begin{aligned} \sum_{s=0}^{S} C^{(q,s)} \overline{P}^{\overline{T}}(t) = \beta \sum_{s=0}^{S} \left[(2s-1)^{-1} F^{(q,s)} - (2s+3)^{-1} F^{(q,s)} \right] \overline{P}^{\overline{T}}(t) \\ -\lambda \sum_{s=0}^{S} \left[(2s-1)^{-1} C^{(q,s)} - (2s+3)^{-1} C^{(q,s)} \right] \overline{P}^{\overline{T}}(t) \\ + (1-\lambda) C^{(q)}(0) + \beta F^{(q)}(0) \end{aligned} \tag{3.41}$$

where $C^{(q)}(0)$ and $F^{(q)}(0)$ are provided or calculated from the previous time interval. Multiplying Equation (3.41) by the shifted Legendre polynomials and integrating yields a system of equations for the $S+1$ coefficients $C^{(q,s)}$. This system forms a tridiagonal matrix equation that can be easily inverted using Gaussian elimination. Because Equation (3.41) depends on flux solution through the fission rate, the delayed neutrons must be solved simultaneously with the response equation. This may be done using feedback iterations outside the response solution.

CHAPTER 4

SOLUTION ALGORITHM

To summarize the previous chapter, the time-dependent coarse-mesh transport consists of solving a set of response equations over a coarse partition of the reactor phase space in a finite time interval. Approximate solutions of the response equations are obtained by projections onto polynomial spaces spanned by combinations of shifted Legendre polynomials. This formulation permits a convenient decoupling of the global problem into a sequence of local (coarse-mesh) transport problems that are characterized by response functions that can be calculated independently of the other local problems. As a result, the computational process can be divided into two phases:

1. Pre-computation: calculation of the response function coefficients for each coarse mesh;
2. Solution construction: coupling of the coarse meshes in space, angle and time by a deterministic algorithm.

This divided approach is very well suited for reactor problems because reactors are often modeled using only a finite number of unique fuel assemblies. Choosing a single fuel assembly as a coarse-mesh therefore means that one is able to reconstruct a full-core solution using only a relatively small number of response functions. The efficiency of this approach has been demonstrated in the steady-state work on this topic.

In this chapter, the implementation of both of these phases will be discussed in the time-dependent context. First the pre-computation (response function generation) phase

will be discussed. Following previous work, the Monte Carlo method will be used. Second, an algorithm for the reconstruction of the global problem will be presented.

4.1 Response Function Generations

Response function calculations require the solution of the transport equation over a single coarse mesh in space, angle and time. Given the derivation of the response functions in Chapter 3, the transport solution method chosen for this task should be capable of the following:

- Modeling continuous surface and volumetric source distributions that vary like the shifted Legendre polynomials in the space and angle variables;
- For calculating the time-responses, one should be able to measure the time distribution of responses initiated at discrete points in time; and
- For all responses, it should be convenient to accurately calculate the response coefficients which are functionals of the angular flux integrated both over surfaces and within the mesh volume.

While it is possible to perform these calculations using deterministic methods (e.g. discrete ordinates with discrete Legendre polynomials(Mosher and Rahnema 2006)), the Monte Carlo method lends itself very naturally to satisfying all three of the above requirements(Forget and Rahnema 2005):

- Monte Carlo methods are able to sample from continuous source distributions of arbitrary shape;
- Source particles may be started at any point in time, and calculating the time elapsed from neutron creation is simple because of the collision-to-collision tracking that Monte Carlo simulations use; and

- The Monte Carlo method is by definition an integral method because of its probabilistic approach.

Previous work (Spanier 1999; Griesheimer, Martin et al. 2005; Griesheimer, Martin et al. 2006) has already established the theoretical and practical grounds for estimating the coefficients of orthogonal expansions, and there is no need to repeat that work here. Previous work (Forget 2006) has also established the theory for sampling from continuous Legendre polynomial distributions.

To adapt the steady-state response function generation methodology to time-dependent response function generation, one samples source particles from the continuous space and angle distributions as usual, but the time of the particle birth is set to zero at the beginning of each neutron track. Then whenever a contribution is made to a response function coefficient estimator (tally), the score is modified to include the appropriate Legendre polynomial evaluated at the time of that event. In the case of track-length tallies for space expansions, the mean value of the Legendre polynomial over the neutron track is calculated and scored.

It should be noted that in steady-state COMET, only the surface-to-surface partial current response functions were required because there was only spatial coupling of the coarse meshes. In time-dependent COMET, as will be discussed in the next section, there is also the need for coupling local problems in time. This requires the addition of surface-to-volume and volume-to-volume angular flux response functions and volume-to-surface partial current response functions. For the calculation of the latter two response functions, the local problem must be solved with a volumetric source. The number of local transport solutions therefore doubles from the steady-state case.

4.2 COMET Solution

For ease of notation, the linear algebraic response equation (3.37)-(3.39) will be written in condensed matrix-vector notation as

$$\boldsymbol{\psi}_n = \mathbf{R}^n_{n-1}\mathbf{j}^+_{n-1}(z_{n-1}) + \mathbf{R}^n_{n+1}\mathbf{j}^+_{n+1}(z_n) + \mathbf{V}^{-1}\mathbf{R}^n_n\boldsymbol{\psi}^0_n, \tag{4.1}$$

$$\mathbf{j}^+_n(z_{n-1}) = \bar{\mathbf{R}}^{n-1}_{n-1}\mathbf{j}^+_{n-1}(z_{n-1}) + \bar{\mathbf{R}}^{n-1}_{n+1}\mathbf{j}^+_{n+1}(z_n) + \mathbf{V}^{-1}\bar{\mathbf{R}}^{n-1}_n\boldsymbol{\psi}^0_n, \tag{4.2}$$

$$\mathbf{j}^+_n(z_n) = \bar{\mathbf{R}}^{n}_{n-1}\mathbf{j}^+_{n-1}(z_{n-1}) + \bar{\mathbf{R}}^{n}_{n+1}\mathbf{j}^+_{n+1}(z_n) + \mathbf{V}^{-1}\bar{\mathbf{R}}^{n}_n\boldsymbol{\psi}^0_n, \tag{4.3}$$

where $\mathbf{V}_g = \text{diag}\{v_g\}$ and $n = 1,...,N$. These equations are approximate forms of the original integral response equations (3.20)-(3.21) over the time interval $[0,T]$.

If the total time interval of interest is $[0,mT]$ for some integer *m*, then Equations (4.1)-(4.3) will be solved within each interval $\left[jT,(j-1)T\right]$ for $j = 0,1,...,m-1$. The initial value of the first interval, $\boldsymbol{\psi}^0_n$, is assumed to be given; for reactor calculations this will typically be the critical flux distribution while for fixed-source problems this will be initial flux condition. The initial value for the second interval, call it $\boldsymbol{\psi}^1_n$, should be the flux distribution evaluated at the end of the first time interval. Equations (4.1)-(4.3) are then solved using this initial source, and the process repeats for all m time intervals.

Within each time interval, Equations (4.1)-(4.3) are solved iteratively. Because these equations are approximate forms of the original integral response equations, a simple Picard iteration(Linz 1985) is used. Using this scheme, Equations (4.1)-(4.3) can be written

$$\boldsymbol{\psi}^{[k+1]}_n = \mathbf{R}^n_{n-1}\mathbf{j}^{+,[k]}_{n-1}(z_{n-1}) + \mathbf{R}^n_{n+1}\mathbf{j}^{+,[k]}_{n+1}(z_n) + \mathbf{V}^{-1}\mathbf{R}^n_n\boldsymbol{\psi}^0_n, \tag{4.4}$$

$$\mathbf{j}^{+,[k+1]}_n(z_{n-1}) = \bar{\mathbf{R}}^{n-1}_{n-1}\mathbf{j}^{+,[k]}_{n-1}(z_{n-1}) + \bar{\mathbf{R}}^{n-1}_{n+1}\mathbf{j}^{+,[k]}_{n+1}(z_n) + \mathbf{V}^{-1}\bar{\mathbf{R}}^{n-1}_n\boldsymbol{\psi}^0_n, \tag{4.5}$$

$$\mathbf{j}_n^{+,[k+1]}(z_n) = \overline{\mathbf{R}}_{n-1}^{n}\mathbf{j}_{n-1}^{+,[k]}(z_{n-1}) + \overline{\mathbf{R}}_{n+1}^{n}\mathbf{j}_{n+1}^{+,[k]}(z_n) + \mathbf{V}^{-1}\overline{\mathbf{R}}_{n}^{n}\boldsymbol{\psi}_n^0 . \tag{4.6}$$

for $k = 1, 2, \ldots$ until convergence.

The convergence criterion for both the flux and the current coefficients is a relative L_2 norm of the difference between the solutions of iterates *k* and *k + 1*. For example, recalling that

$$\psi_{n,g}(x,t) \approx \psi_{n,g}^{(Q,R,S)}(x,t) = \sum_{s=1}^{S}\sum_{q=0}^{Q}\sum_{r=0}^{R}\psi_{n,g}^{0,(q,r)}(t)P_{qr}^{\Re_n}(x)\overline{P}_s^{\overline{T}}(t)$$

the angular flux criterion, for example, can be written

$$\begin{aligned}
\tau &> \max_{n,g}\left\{\frac{\int_0^T\int_{\Re_n}\left[\psi_{n,g}^{(Q,R,S),[k+1]}(x,t) - \psi_{n,g}^{(Q,R,S),[k]}(x,t)\right]^2 dxdt}{\int_0^T\int_{\Re_n}\left[\psi_{n,g}^{(Q,R,S),[k]}(x,t)\right]^2 dxdt}\right\} \\
&= \max_{n,g}\left\{\frac{\int_0^T\int_{\Re_n}\left[\sum_{s=1}^{S}\sum_{q=0}^{Q}\sum_{r=0}^{R}\left(\psi_{n,g}^{(q,r,s),[k+1]} - \psi_{n,g}^{(q,r,s),[k]}\right)P_{qr}^{\Re_n}(x)\overline{P}_s^{\overline{T}}(t)\right]^2 dxdt}{\int_0^T\int_{\Re_n}\left[\sum_{s=1}^{S}\sum_{q=0}^{Q}\sum_{r=0}^{R}\psi_{n,g}^{(q,r,s),[k]}P_{qr}^{\Re_n}(x)\overline{P}_s^{\overline{T}}(t)\right]^2 dxdt}\right\} \\
&= \max_{n,g}\left\{\left(\frac{\sum_{s=1}^{S}\sum_{q=0}^{Q}\sum_{r=0}^{R}\frac{\psi_{n,g}^{(q,r,s),[k+1]} - \psi_{n,g}^{(q,r,s),[k]}}{(2q+1)(2r+1)(2s+1)}}{\sum_{s=1}^{S}\sum_{q=0}^{Q}\sum_{r=0}^{R}\frac{\psi_{n,g}^{(q,r,s),[k]}}{(2q+1)(2r+1)(2s+1)}}\right)^2\right\}
\end{aligned} .$$

This criterion effectively weights the moments by approximately the inverse of their degree, resulting in more weight being associated with low order, dominant coefficients and less weight being associated with the high order, potentially noisy moments. Previous COMET work has used criteria based only on the zeroth order moments because calculating coefficient-by-coefficient relative changes for small, high-order coefficients is not a reliable measure of convergence.

Recall that length of the $\boldsymbol{\psi}_n$ vector is $G(Q+1)(R+1)(S+1)$ and the length of the $\mathbf{j}_n^{\pm}$ vectors are $G(Q+1)(S+1)$. The system of equations therefore has the potential to become quite large as expansion orders increase. A few observations lead to increased efficiency of these iterations:

- The terms $\mathbf{V}^{-1}\mathbf{R}_n^n\boldsymbol{\psi}_n^0$, $\mathbf{V}^{-1}\overline{\mathbf{R}}_n^n\boldsymbol{\psi}_n^0$ and $\mathbf{V}^{-1}\overline{\mathbf{R}}_n^n\boldsymbol{\psi}_n^0$ (i.e. the initial value terms) only need to be evaluated once per time interval because they are not a function of the solution in that time interval;
- The vector $\boldsymbol{\psi}_n^{[k+1]}$ only needs to be evaluated to compute the initial value for the next step;
- The iterations within each time interval function to couple the meshes in space, angle and time, which can be accomplished through the computation of the $\mathbf{j}_n^{+,[k+1]}$ vectors alone.

Because of the last two points, the iterations only need to be performed with Equations (4.5) and (4.6) initially. Once the $\mathbf{j}_n^{+,[k+1]}$ vector is converged, Equation (4.4) is included in the iteration and $\boldsymbol{\psi}_n^{[k+1]}$ should already be nearly converged based on the convergence of the $\mathbf{j}_n^{+,[k]}$.

CHAPTER 5

NUMERICAL RESULTS

Four example problems are studied in following section. Each problem is intended to focus on a different aspect of the new time-dependent method. These examples are roughly in order of increasing complexity. In each section, the example problem will be described, and it will be noted which aspect of the time-dependent theory is designed to highlight. The final example is a heterogeneous reactor problem and represents the sum of all of the components of the new theory.

5.1 Olson-Henderson Slab

The first problem that will be considered is a homogeneous, finite slab. The slab initially has no neutrons, and at time $t = 0$ a uniform, isotropic source is "turned on" and remains on for the duration of the problem, eventually evolving to a steady-state distribution. The slab is ten mean-free-paths in width with vacuum boundary conditions and is not fissionable; the ratio of the scattering to the total cross section is 0.9. This problem was chosen because there is an analytical solution available in the literature (Olson and Henderson 2004). This problem will test both the time-stepping procedure and the convolution approximation described in the Chapter 3.

Figure 1 shows the analytical, COMET and discrete ordinates (S_{32}) flux solutions as a function of space at 1.0, 2.5, 5.0, 7.5 and 10 mean-free-times. The COMET solution was generated using a 5^{th} order angular expansion, 10^{th} order spatial expansion and 10^{th} order time expansion. It can be seen that the solutions differ the most near the slab boundaries, particularly at later times.

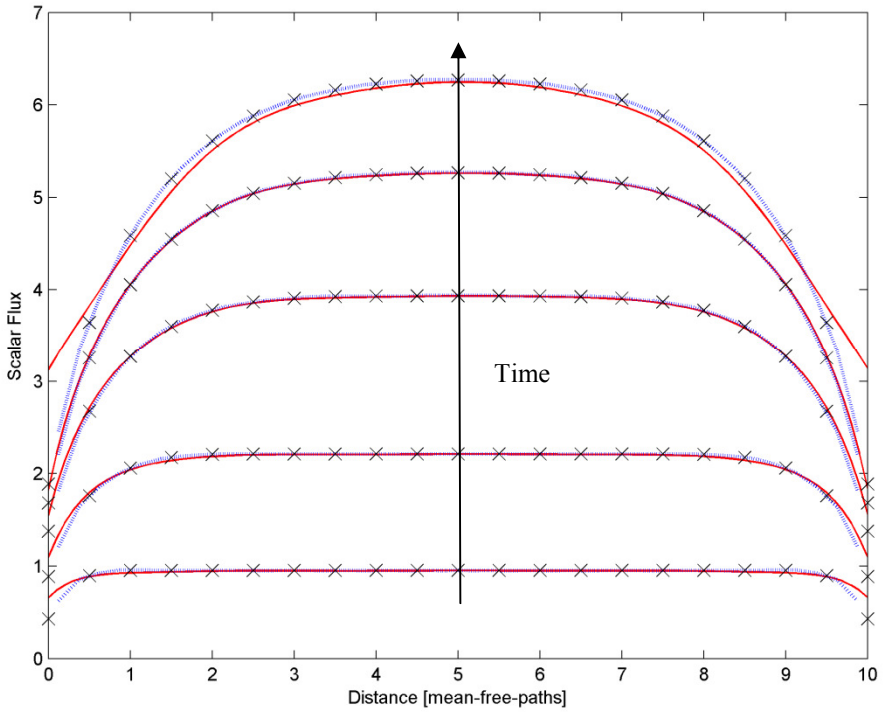

Figure 1: Example 1, analytical (crosses), discrete ordinates (blue) and COMET (red) flux distributions; solutions shown at $t = 1.0, 2.5, 5.0, 7.5, 10$ mean-free times

5.2 Infinite Medium Example

A problem will now be examined that is infinite and homogeneous in the spatial dimension. Although the problem is physically an infinite medium, it is modeled in COMET as a finite slab with specular reflection boundary conditions to verify the theory and the implementation of the new time-dependent theory.

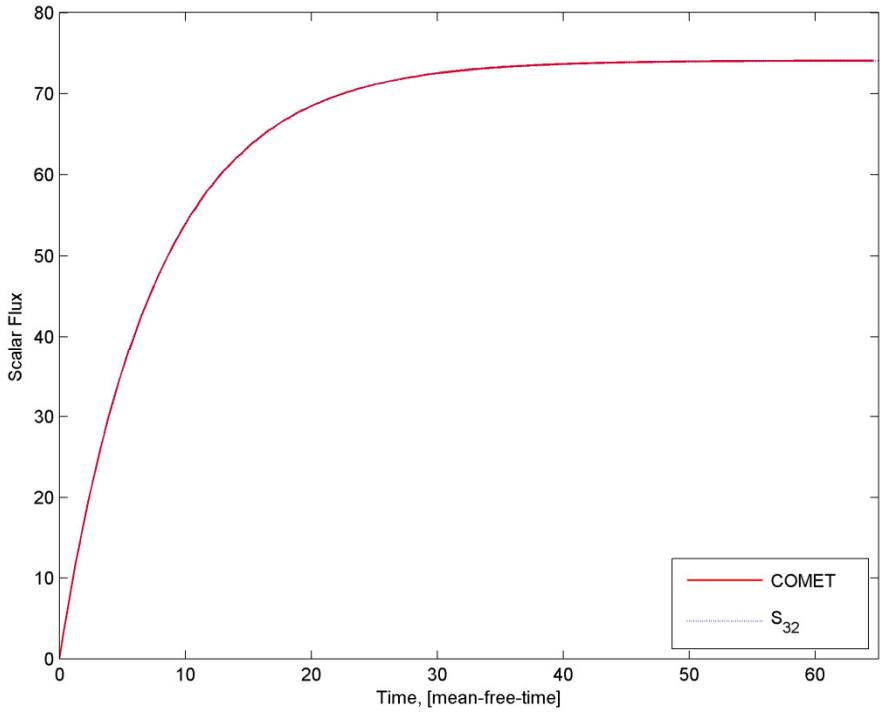

Figure 2: Flux evolution to steady state, dt=1.0 mft

In an infinite medium with isotropic scattering and no external source of anisotropic neutrons, the transport equation is invariant with respect to space and angle, resulting

$$\frac{1}{v}\frac{\partial \psi(t)}{\partial t} + \bar{\sigma}\psi(t) = 0$$

where $\bar{\sigma} \equiv \left(\sigma - \sigma_s - \nu\sigma_f\right)$ and an condition $\psi(0) = \psi_0$ is prescribed. The solution of this equation is a simple exponential

$$\psi(t) = \psi_0 e^{-v\bar{\sigma}t}.$$

The time interval considered is [0, 42]. For $t \in [0, 21]$ the system is made super-critical with a $k_\infty = 1.100$; for $t \in [21, 42]$ a negative reactivity is inserted by increasing absorption so that $k_\infty = 0.900$. Figure 3 shows the converged COMET solutions with time steps equal to 7 and 21 using a 15th order time expansion (the results are accurate enough that the plots are visually indistinguishable). Table 1 shows the average (AVG), root-mean-square (RMS) and maximum (MAX) errors of the scalar flux solution over a finely spaced uniform grid. The maximum errors in all cases occur at the time-step boundaries.

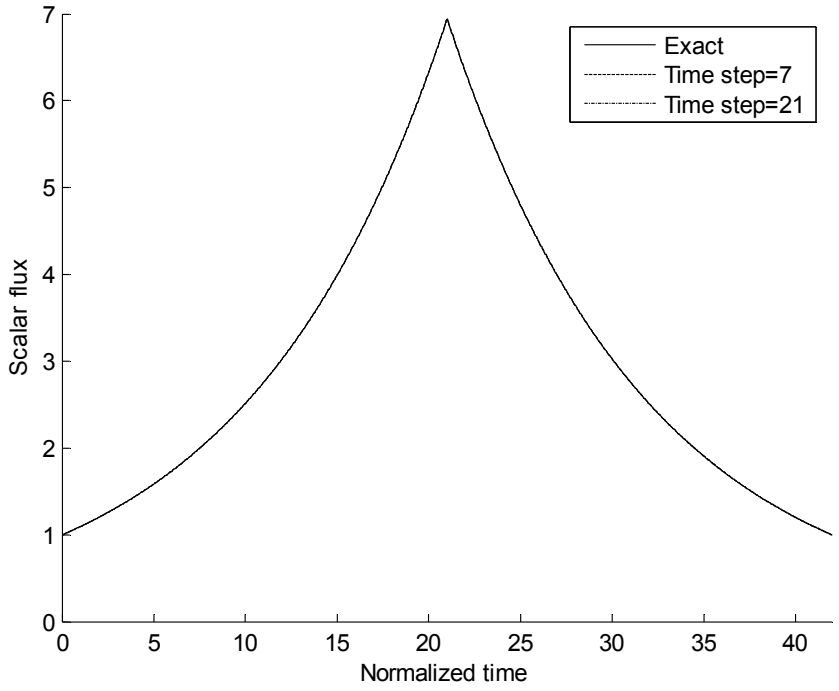

Figure 3: Example 2, plot of scalar flux vs. time for exact solution and 15th order response-based solutions with time steps equal to 7 and 21

Table 1: Example 2, Average Scalar Flux Error Statistics

Time step width	Exp. Order	AVG	RMS	MAX
7	5	0.31%	0.41%	1.65%
	10	0.06%	0.07%	0.14%
	15	0.05%	0.05%	0.08%
21	5	5.09%	8.70%	37.21%
	10	0.31%	0.44%	1.86%
	15	0.07%	0.09%	0.38%

5.3 Semi-Infinite Medium With Time-Varying Incident Source

A semi-infinite medium $\left(z \in [0,\infty]\right)$ with an oscillating impinging current, $\Gamma_0(t) = 1 + \sin \omega t$, is studied in this example. Because this is an infinite-medium fixed-source problem, there is no volumetric initial source, and the only response that needs to be calculated is the exiting partial currents. The response equations therefore simplifies to

$$j^+(x_0,t) = \int_0^t dt' \int_{\partial \Re^+} dx' \Gamma_0(x',t') \bar{G}_n^{g' \to g}(x' \to x_0, t' \to t),$$

which has the following approximate form *a la* Chapter 3:

$$\mathbf{j}^{(q)+}(z_0) = \sum_{q'=0}^{Q} \bar{\mathbf{R}}_{q'}^{q} \boldsymbol{\Gamma}_0^{(q')}(z_0).$$

The time-expansion coefficients of the incident source were calculated using the adaptive-recursive Simpson's rule in MatLab®. This example primarily serves to test the approximation of the surface-to-surface time-convolution approximation.

Figure 4 shows the solution using an 11^{th} order time-expansion and a histogram plot of the MCNP (2003) Monte Carlo reference solution. Table 2 presents the average (AVG), root-mean-square (RMS) and maximum (MAX) errors of the solution integrated over each of the MCNP time bins.

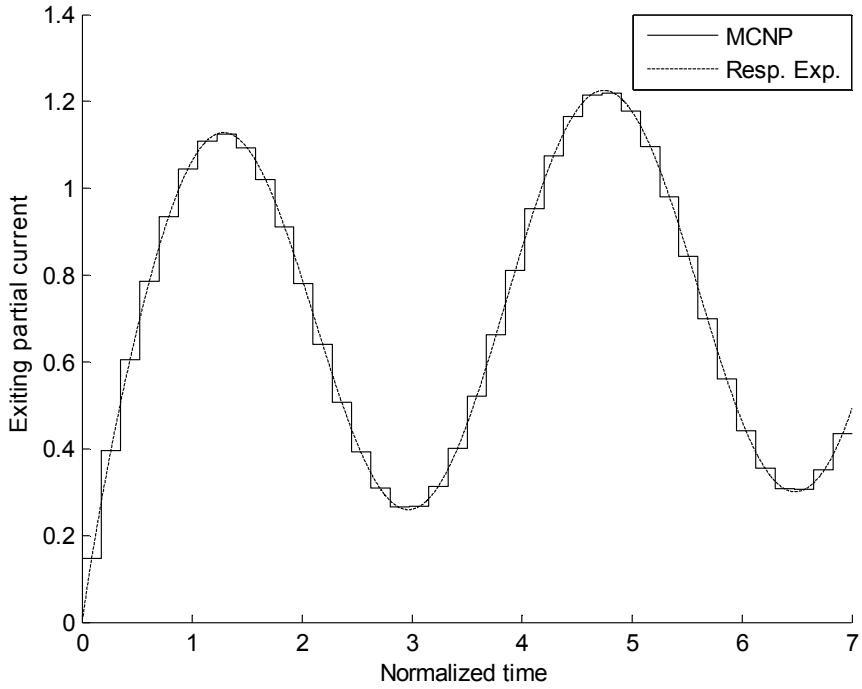

Figure 4: Example 3, plot of 11^{th} order response solution and MCNP reference solution histogram

Table 2: Example 3, Bin-Integrated Error Statistics

Expansion order	AVG	RMS	MAX
8	2.76%	3.60%	8.34%
11	0.14%	0.18%	0.41%
14	0.02%	0.03%	0.08%
17	0.02%	0.03%	0.09%

5.4 ANL Fast Reactor Benchmark

In this last example, a 2-group heterogeneous fast reactor benchmark based on Benchmark 16 from the Argonne National Laboratory Benchmark Problem Book (1985) is examined. This problem is the more realistic example in terms of heterogeneity, and fully utilizes all of the theory developed in Chapter 3.

The reactor consists of seven homogeneous regions that are summarized in Table 3. The solutions presented here include prompt neutrons only. The initial critical flux distributions are shown in Figure 6. The discrete ordinates solution uses 32-point Gauss-Legendre quadrature in angle and a finite difference scheme spatially; the COMET solution uses an 8^{th} order angular expansion and 15^{th} order expansion in space. The eigenvalues are shown in Table 4.

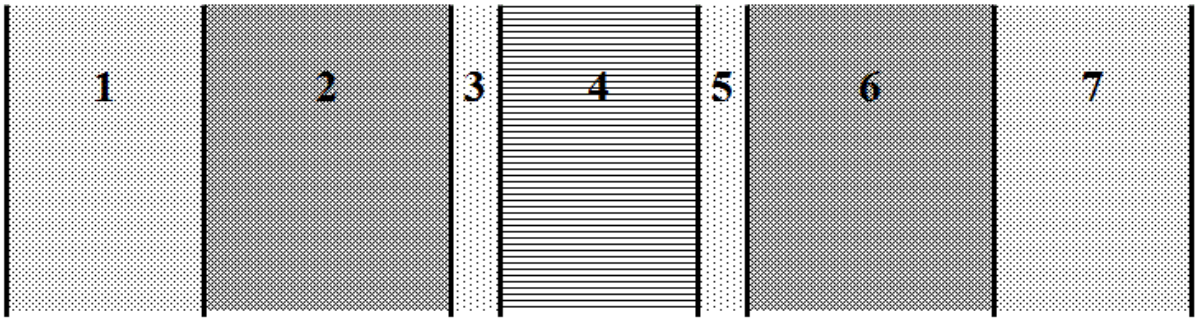

Figure 5: ANL Benchmark 16 Geometry

Table 3: ANL Benchmark Characteristics

Zone	Material	Width [cm]	$\nu\sigma_{f,1}/\sigma_1$	$\nu\sigma_{f,2}/\sigma_2$	$\sigma_{a,1}/\sigma_1$	$\sigma_{a,2}/\sigma_2$
1, 7	Blanket	40.000	3.461E-03	7.856E-04	1.600E-02	2.444E-02
2, 6	Outer Core	47.374	4.030E-02	3.016E-02	2.760E-02	3.566E-02
3, 5	Control Rod	9.000	0.000E+00	0.000E+00	7.308E-02	8.693E-02
6	Inner Core	34.000	4.030E-02	3.016E-02	2.760E-02	3.566E-02

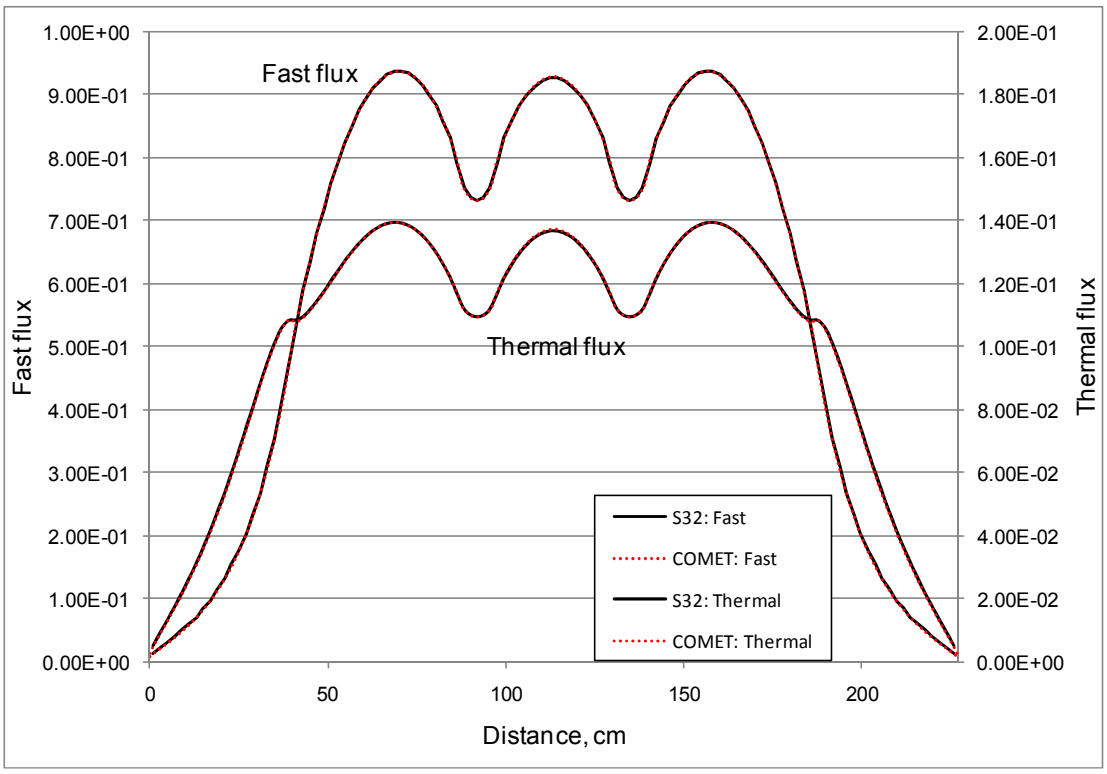

Figure 6: ANL Benchmark Critical Flux Configuration

Table 4: Example 4, Eigenvalue Comparison

	k_{eff}	Δk_{eff}
S32	0.999807	74.4×10^{-5}
COMET	1.000551	

At time $t = 0$, a transient is initiated by increasing the density of zone 2 by 10%. The subsequent evolution of the multigroup fluxes was calculated by 32-point discrete ordinates with implicit differencing on the one hand, and COMET with the 8^{th} order angular, 15^{th} order spatial and 15^{th} order time expansions. The discrete ordinates time step was 10^{-8} seconds; two COMET solutions were computed, one with a time step (i.e.

the width of the time expansion interval) of 5×10^{-7} seconds the other with a time step of 2×10^{-6} seconds. The total neutron production rate $\left(\sum_{g'=1}^{2}\nu\sigma_{f,g}\phi_g(t)\right)$ resulting from these calculations is plotted in Figure 7.

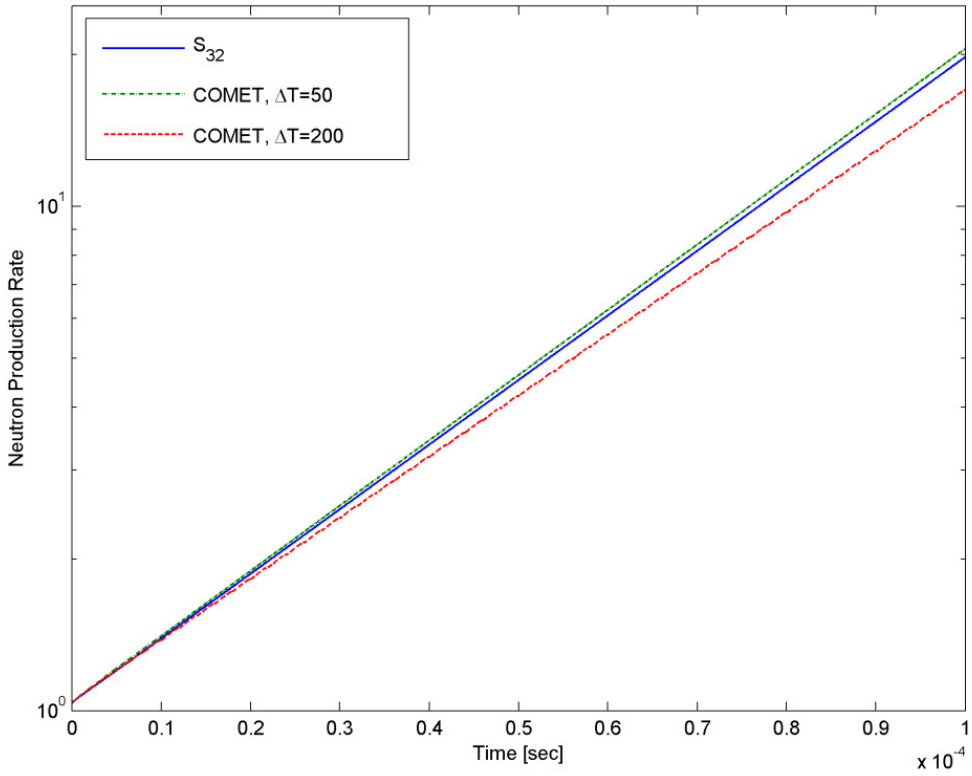

Figure 7: Total neutron production rate for $t\in\left[0,10^{-4}\right]$

The agreement between COMET and discrete ordinates is quite good when the expansion time interval is 5×10^{-7} with a maximum error of 3.7% at 10^{-4} seconds; the longer time step, however, delivers an error of 13.8% at the same point. This seems to

imply that the 8/15/15 expansion orders are insufficient in capturing the responses over this time scale.

It is important to recall that the order of the time expansion is dictated by the behavior of the individual responses—not of the final solution. The time-behavior of the responses can vary greatly depending on factors like the opacity and size of the mesh. For example, Figures 8-9 show the surface and volume response components contributing to the total fluxes in the right half of zone 2 (fuel material) and in zone 3 (control material). In these figures, the "Volume component" is the contribution to the total time-dependent flux from the initial source; the "Surface component" is the component of the total flux resulting from incoming boundary sources.

Figure 10 shows the neutron production rate on the tighter scale $[0,10^{-5}]$. From this plot one immediately notices small 'hiccups' in the short-time-step solution and higher-order noise in the long-time-step solution that create seemingly random fluctuations about the discrete ordinates solution. This effect is investigated visually in Figures 11-13, which show the group fluxes in the right half of zone two (core material), in zone 3 (the control rod), and in the left half of zone 4 (core material). The expansion time interval in these figures is 5×10^{-7}, and the time step boundaries are noted with vertical dashed lines.

These figures reveal two phenomena: (1) wave-like perturbations in the flux at the beginning of all but the first time step and (2) high-order oscillations peaking near the time interval boundaries. The amplitude and shape of the wave-like perturbations vary throughout the core, but are most pronounced in the scalar flux in the control rod. The

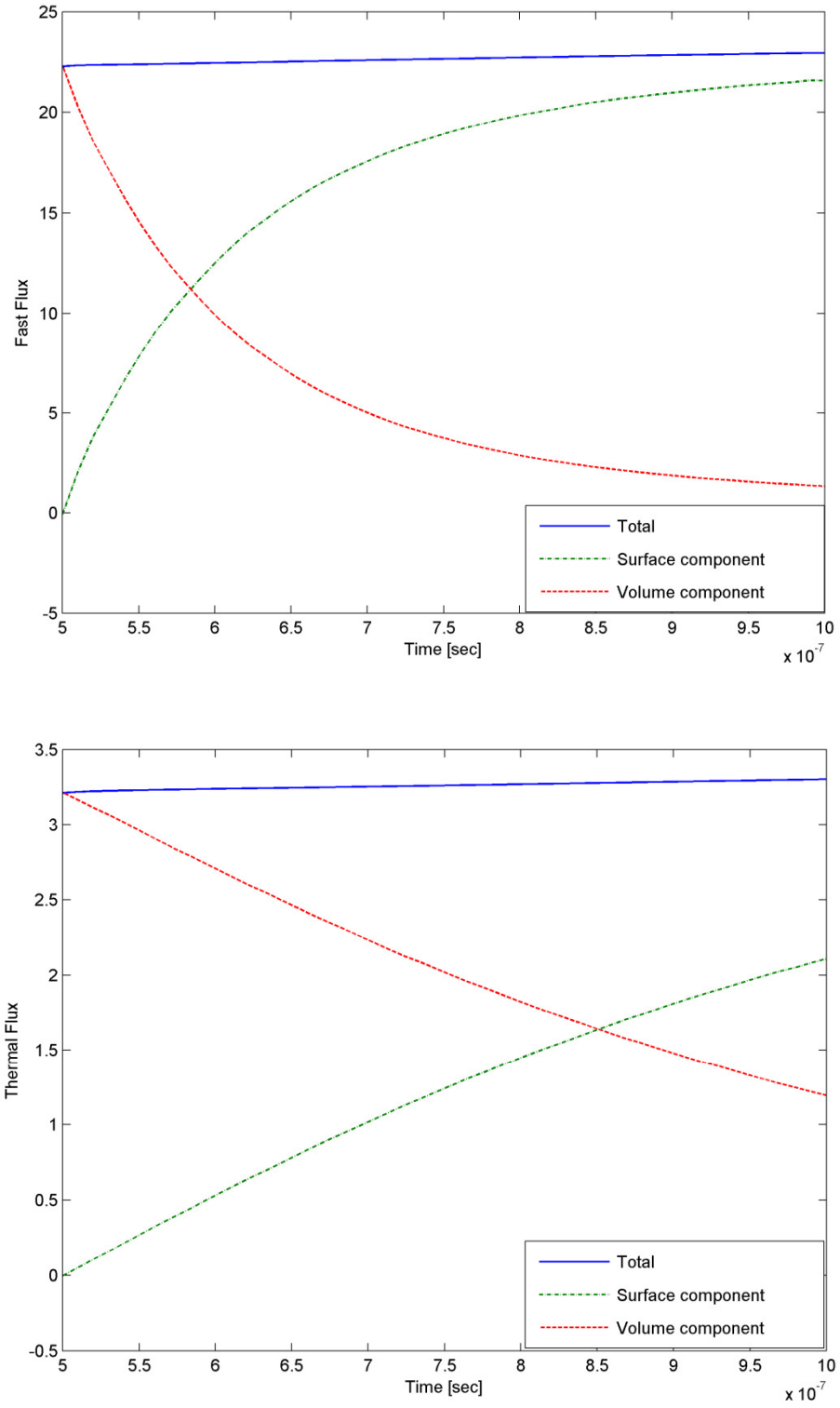

Figure 8: Scalar Flux Response Components In the Right Half of Zone 2; (TOP) fast flux, (BOTTOM) thermal flux

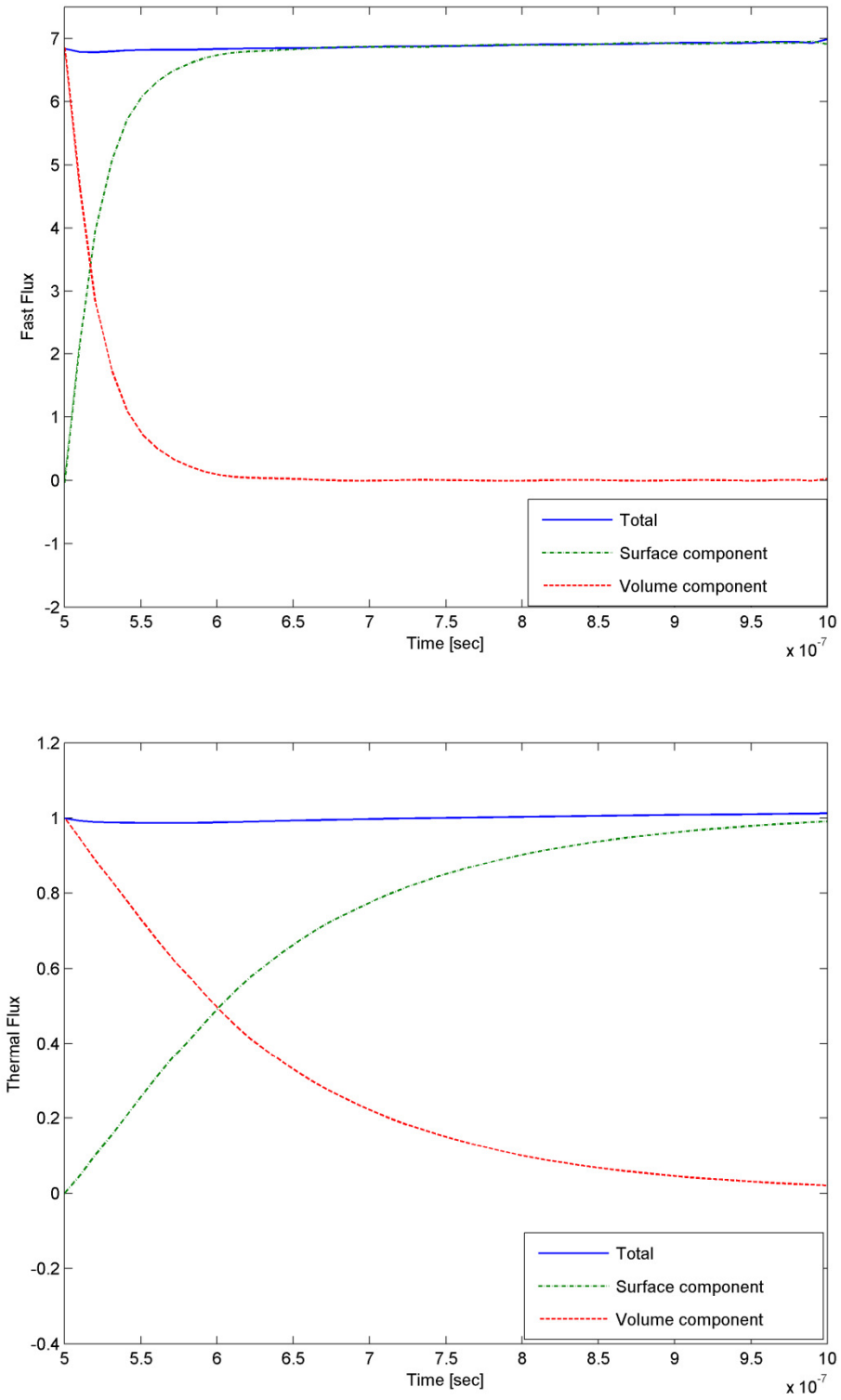

Figure 9: Scalar Flux Response Components In the Right Half of Zone 2
(TOP) fast flux, (BOTTOM) thermal flux

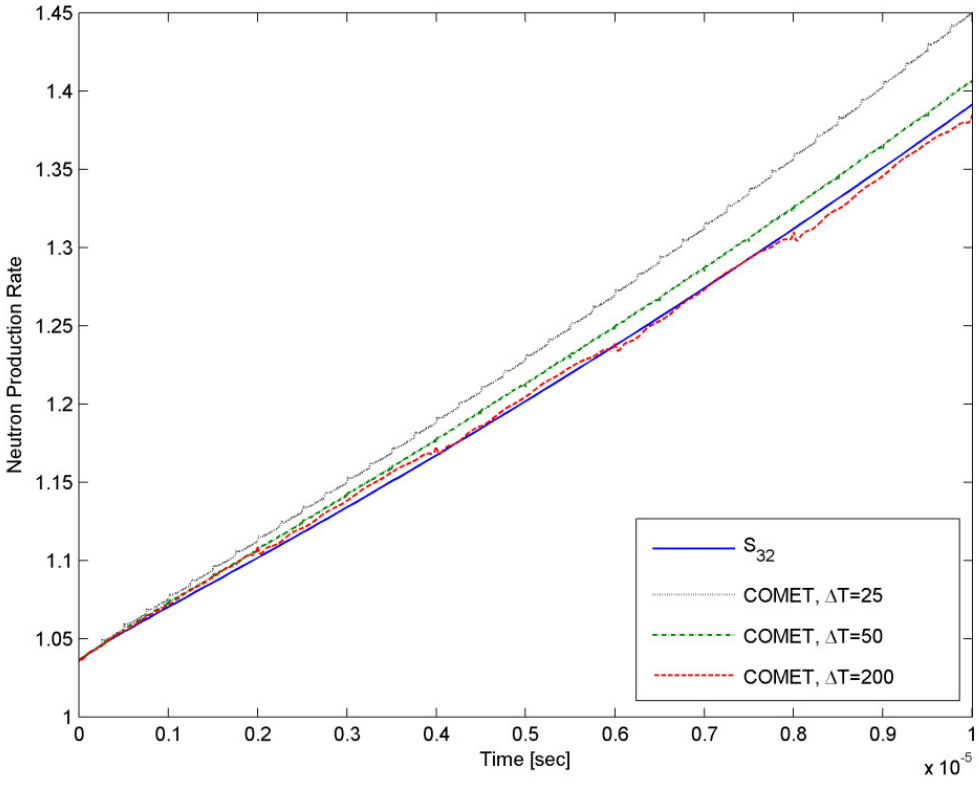

Figure 10: Total neutron production rate for $t \in \left[0, 10^{-5}\right]$

scalar flux at each time-step boundary is continuous, and the perturbation appears a very short time into the new time mesh—it does not begin exactly at the time boundary. The numerical procedure for transitioning from one time step to the subsequent step can be summarized as follows:

1. the space-angle-time expansion of the angular flux in each spatial coarse mesh is calculated by summing the response components from the bounding surfaces and from the initial value;
2. this expansion is evaluated at the time corresponding to the end of the current time step;

3. the space-angle expansion resulting from step 2 becomes the initial value of the next time-step.

It is hypothesized that the transition from step 2 to step 3 is causing the observed perturbation by creating temporary particle imbalances near the coarse mesh surfaces. Specifically, slow convergence and the truncation error of the flux expansion near the space and time boundary points create local instabilities (manifested as particle imbalances) that are transferred to the next time step. Once in the subsequent time step, these local perturbations, which exist most dominantly just inside the coarse mesh boundaries, give rise to small transients created by localized excesses or deficiencies of neutrons. This hypothesis is supported by two observations. First, within each time interval the initial source term has decay-like behavior in time: its contribution to the total flux within that mesh decrease at a sharp rate as the initial neutrons leak from the mesh or are absorbed. Errors or inconsistencies in the initial value should also manifest this decay-like behavior, which is what is observed numerically. Furthermore, the flux in each time-interval appears to be asymptotically correct because at later times within any given time interval the total flux is dominated by the low-frequency coupling with other nearby meshes. The second piece of evidence is that the initial time step is unaffected. The initial (critical) source for the first time step is at no point subjected to a time-expansion, and convergence of the eigenvalue guarantees particle balance.

The notion of this type of boundary error is further supported by observing the spatial distribution of the flux at discrete time-points. Figure 14 presents the group fluxes at $t = 0, 10^{-6}, 10^{-5}$. The agreement between COMET and discrete ordinates is reasonable except for sharp depressions at the mesh boundaries.

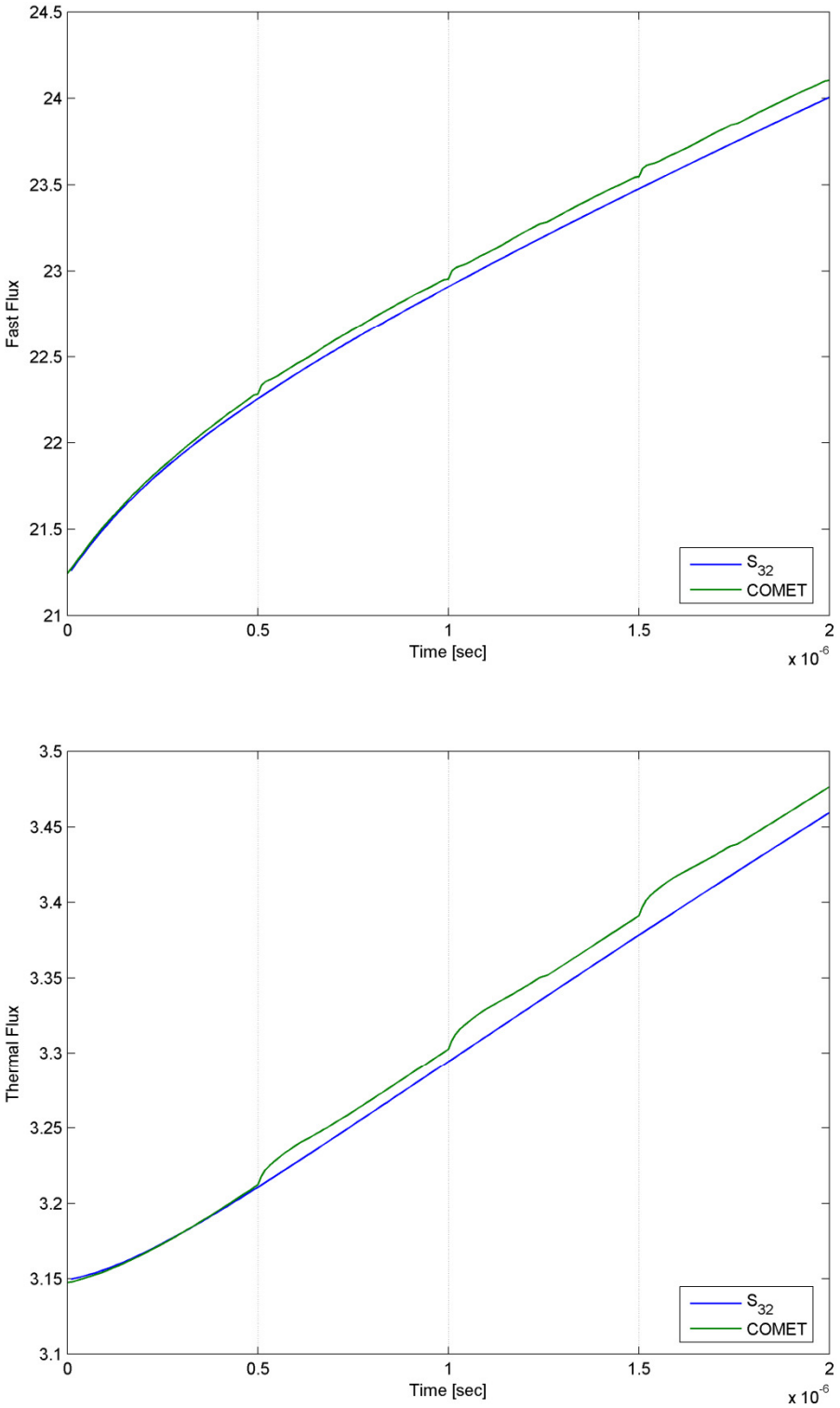

Figure 11: Scalar Fluxes In Right Half of Zone Two;
(TOP) fast flux, (BOTTOM) thermal flux;
Error at 2×10^{-6} : 0.4% (fast) and 0.5% (thermal)

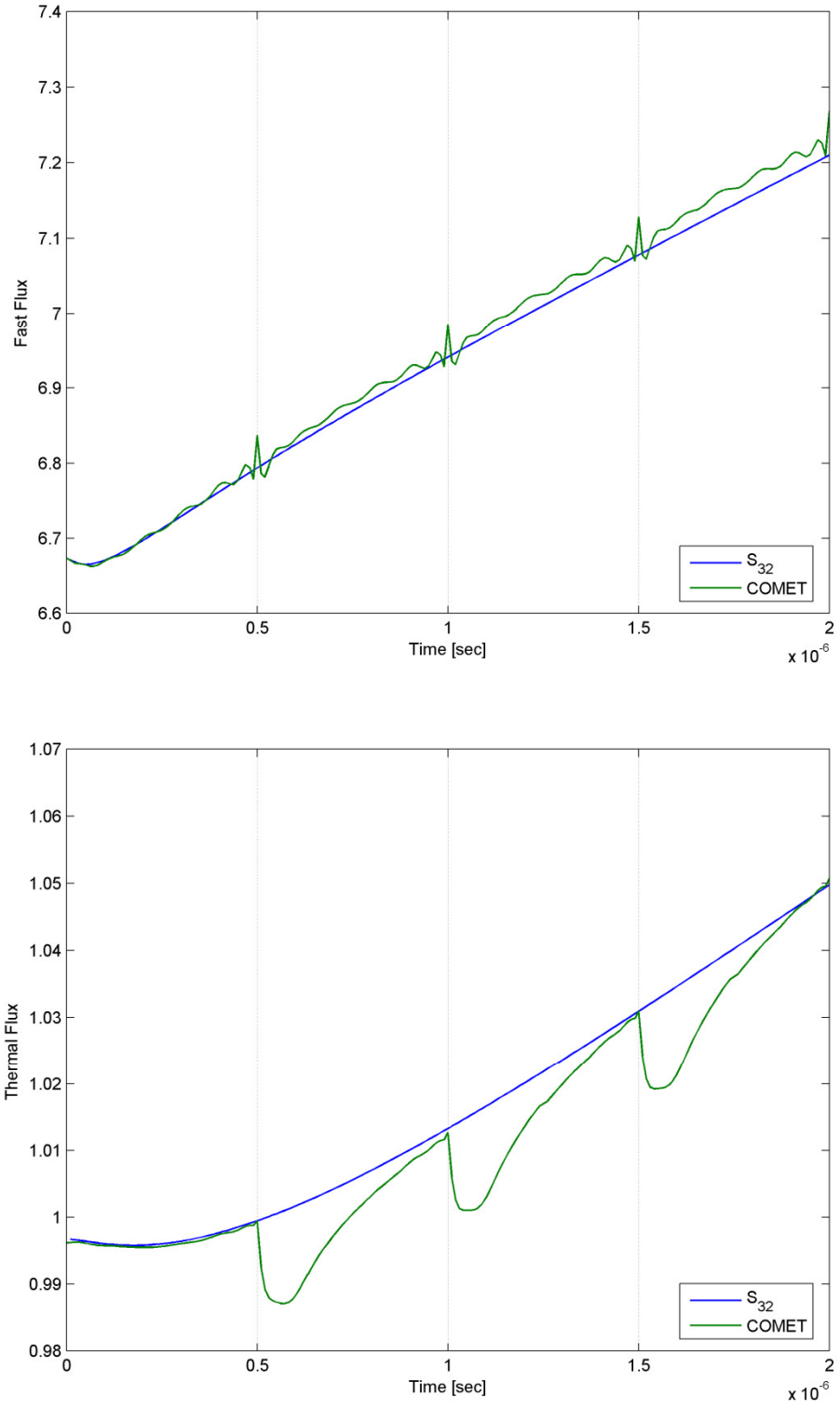

Figure 12: Scalar Fluxes in Zone Three;
(TOP) fast flux, (BOTTOM) thermal flux
Error at 2×10^{-6} : 0.8% (fast) and 0.09% (thermal)

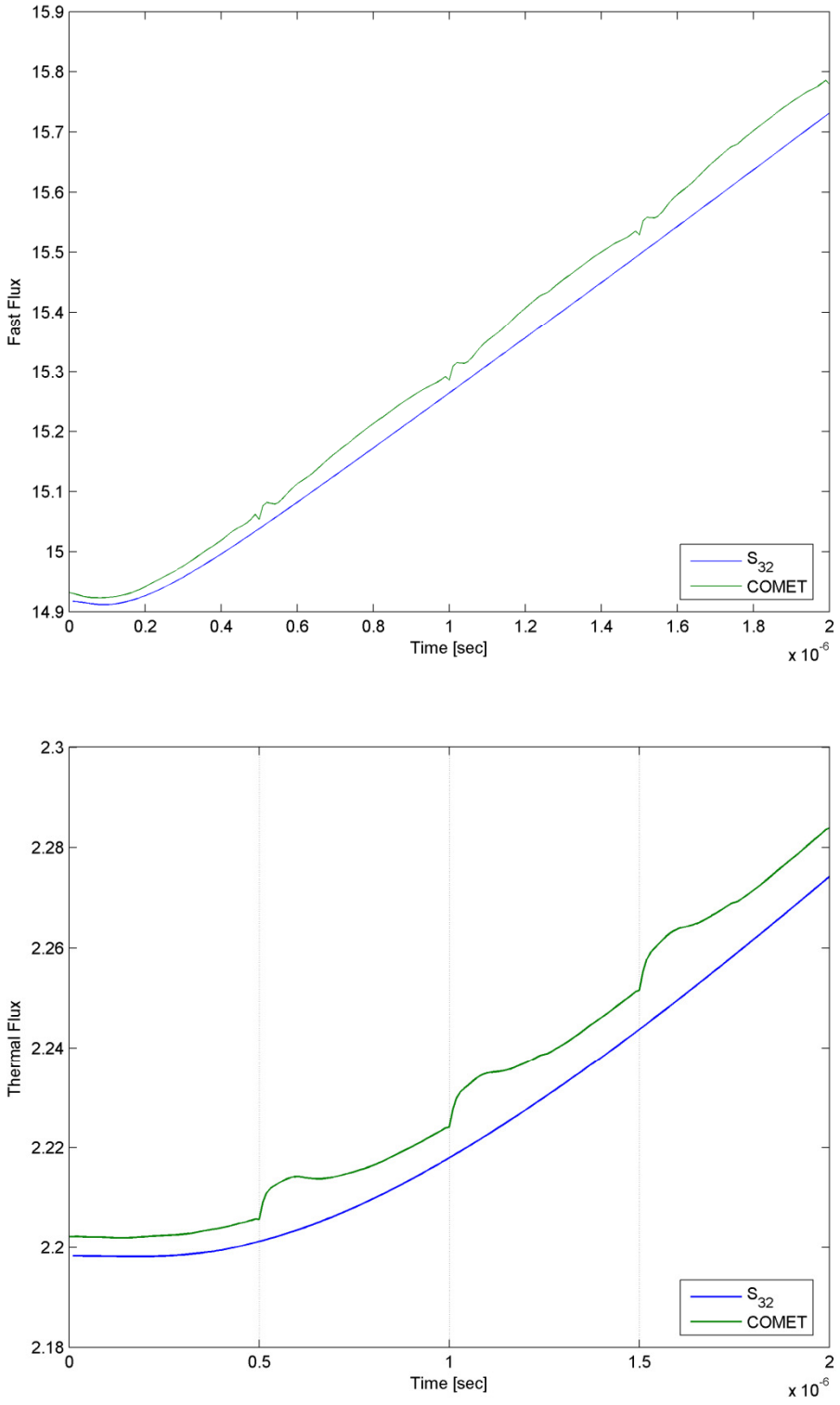

Figure 13: Scalar Fluxes In the Right Half of Zone 4
(TOP) fast flux, (BOTTOM) thermal flux
Error at 2×10^{-6} : 0.3% (fast) and 0.4% (thermal)

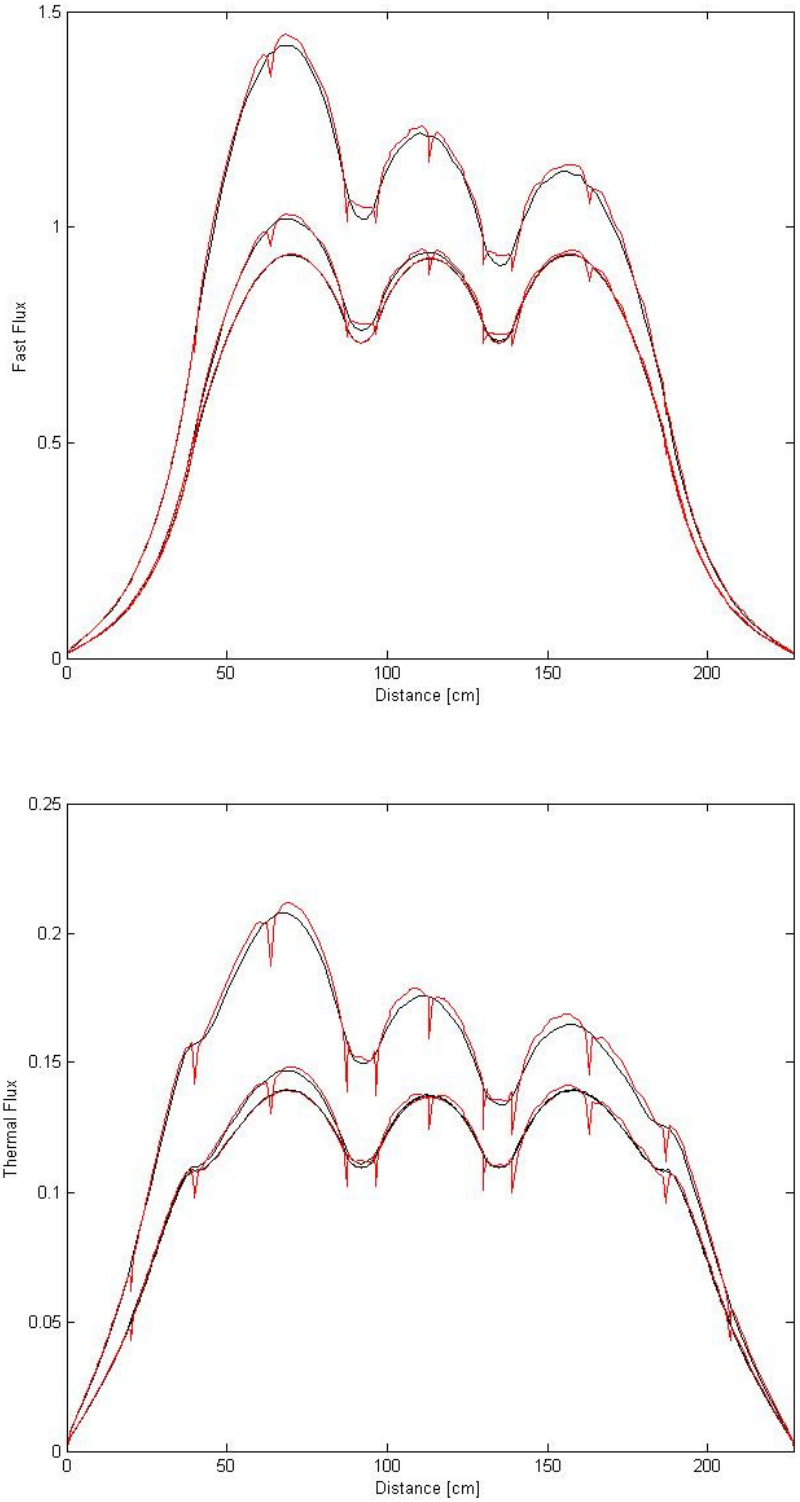

Figure 14: Spatial Flux Distribution at $t = 0, 10^{-6}, 10^{-5}$ Seconds
(TOP) fast flux, (BOTTOM) thermal flux

The second phenomena that can be observed in Figures 11-13 are high order oscillations, particularly in the fast flux. These oscillations result principally from the constraint that the flux be continuous. This constraint is enforced by modifying the highest order coefficients in the time expansion at the end of each time iteration. If this adjustment is positive, then the high order polynomial becomes amplified. In fact, one can see from the figures that the shape of these oscillations is consistent with the order of the expansion.

5.5 Summary

Four example problems have been presented to verify the implementation of the time-dependent coarse-mesh transport method and highlight a few challenges that remain. To summarize:

- The Olson-Henderson slab problem tested the polynomial convolution approximation by computing the volumetric angular flux response from a constant time source. Excellent agreement was seen in the total (integrated) flux as the solution evolved to steady state; point-wise, however, it was seen that even fairly high order polynomial expansions may not accurately reproduce the exact solution near spatial boundaries.
- The infinite-medium problem again tested the polynomial convolution method, this time in a spatially uniform setting. The problem was solved as a finite medium with specular reflection boundary conditions, enabling verification of all time-expanded response functions (surface-to-surface, surface-to-volume, volume-to-surface and volume-to-volume) to zeroth order in space and first order in angle.

- The semi-infinite medium problem tested surface-to-surface response-convolution of a source that oscillated in time. This problem was unique primarily because the surface source was not monotone increasing or decreasing.
- The final example problem solved a more realistic reactor problem with sharp spatial flux gradients and non-uniform perturbations initiating the transient behavior. Reasonable solutions were obtained for the integrated neutron production rate. This problem also revealed the difficulty of representing the time-varying space-angle distribution of using polynomial expansions. A careful analysis of this problem will enlighten future work extending this method.

CHAPTER 6

CONCLUSION

A time-dependent transport theory method has been developed that extends the steady-state coarse-mesh transport method. First, a framework was developed for addressing time-dependence in the governing response equation that forms the basis of the coarse-mesh transport method. The result was a time-dependent response equation that is very general and potentially solvable using various approximation techniques. In this work, the response equation was approximated by projecting the source terms onto polynomial spaces in finite time intervals. Algorithm was then developed based on this approach for theoretically solving large reactor transient problems.

In looking at specific example problems, the new method was shown to be very accurate for fixed-source time-dependent transport problems. A one-dimensional fast reactor problem was also solved that predicted the integral neutron production rate quite well. This last example problem also turned out to be highly valuable in revealing directions which future work must follow to make the new time-dependent method generally applicable for realistic reactor systems with high degrees of heterogeneity and transients initiated by localized perturbations. Some of these future directions will now be discussed in closing.

First, the fast reactor benchmark problem of Section 5.4 highlighted a challenge in coupling the time-dependent response from one time interval to the next. Specifically, evaluating the time-space-angle expansion of the flux at the end of one time interval to be used as an initial value in a subsequent time interval introduces small perturbations in the

subsequent time interval. These perturbations arise from local particle imbalances resulting from the truncation error of the polynomial expansions. Fortunately, the effect of these perturbations seems to decay quite rapidly, but there appears to be an aggregate build up of error when thousands of time steps are taken. It could be argued that increasing the order of the polynomial may resolve this problem, but further increasing the polynomial expansion order would increase the computation time significantly, particularly when the order is increased in the space and angle expansions. Listed below are several alternatives that may improve the accuracy and efficiency of the method.

First, in the current work the interface partial currents are expanded in the angular half-spaces while the volumetric angular flux is expanded in the whole angular space. Expanding the volumetric flux in the angular half spaces would likely increase the accuracy of the flux anisotropy near spatial boundaries/interfaces. This could potentially allow for smoother spatial coupling of coarse meshes.

Second, tighter coupling between time intervals could reduce time interface oscillations. This could be achieved by doubling the response expansion interval to provide a continuous (overlapping) source of neutrons from interval to the next, although the mathematical maneuvering of this scheme might be slightly more challenging.

Third, a lower order polynomial expansion of the response functions (in the time variable) could be achieved if the source were continuous in time rather than a delta function. The delta function response functions would still be required for the response from the initial source, however, the number of total response functions would increase by a factor of two. This increase in the number of response functions would increase the

amount of computer memory required but could lead to faster computations by reducing the size of the total response matrix.

Lastly, the time-dependent response equation is fundamentally an initial-value-type integral equation. This opens the door for using a variety of numerical integral methods. For example, rather than making the error term of the approximate response equation orthogonal to the projection space on each interval, one could use a collocation method that solves the equation exactly at a finite number of points. If the final collocation point was at the time interval point, this approach might also minimize destabilizing error propagation.

In closing, the work presented in this dissertation advances the theory and understanding of the coarse-mesh transport method by developing a generalized framework for solving time-dependent neutron transport problems. The theory developed in the first half of Chapter 3 provides a spring board for investigating various approximations of the time-dependent response equation. One such approximation was presented in the second-half of Chapter 3 that was shown to perform very well in certain contexts. It was shown in Chapter 4 that there exist a few challenges for the time-dependent coarse-mesh transport theory that are unique from other deterministic transport methods. As mentioned above, these challenges can likely be resolved by adapting the approximation space of the solutions. More fundamentally, it is possible that the approach for thinking about time-dependent transport problems taken in this work may be applied to other space-angle discretizations of the transport equation besides the coarse-mesh method. Under other space-angle discretization some of the present challenges

would likely dissipate; investigating this possibility would be an interesting topic for future work.

REFERENCES

(1985). National Energy Software Center: Benchmark Problem Book, Argonne National Laboratory.

(2003). MCNP- A General Monte Carlo N-Particle Transport Code, Version 5, Los Alamos National Laboratory.

Akcasu, Z., G. S. Lellouche, et al. (1971). Mathematical Methods in Nuclear Reactor Dynamics. New York, Academic Press.

Ash, M. (1979). Nuclear Reactor Kinetics. New York, McGraw-Hill International Book Company.

Bell, G. I. and S. Glasstone (1979). Nuclear Reactor Theory. Huntington, NY, Robert E. Krieger Publishing Company.

Bentley, C., R. Demeglio, et al. (1997). Development of a Hybrid Stochastic/Deterministic Method for Transient, Three-Dimensional Neutron Transport. Proceedings of the Joint International Conference on Mathematical Methods and Supercomputing for Nuclear Applications. Saratoga, NY. **2:** 1670-1681.

Chang, R.-Y. and M.-L. Wang (1985). "Solutions of Integral Equations Via Shifted Legendre Polynomials." International Journal of Systems Science **16**(2): 197-208.

Chang, R.-Y., S.-Y. Yang, et al. (1987). "Solution of Integral Equations Via Generalized Orthogonal Polynomials." International Journal of Systems Science **18**(3): 553-568.

Downar, T., D. Lee, et al. (2004). PARCS v2.6: U.S. NRC Core Neutronics Simulator, Purdue University/US NRC.

Dulla, S., E. H. Mund, et al. (2008). "The Quasi-static Method Revisited." Progress in Nuclear Energy **50**: 908-920.

Dulla, S., P. Ravetto, et al. (2005). "Some Features of Spatial Neutron Kinetics for Multiplying Systems." Nuclear Science and Engineering **149**: 88-100.

Forget, B. (2006). A Three Dimensional Heterogeneous Coarse Mesh Transport Method for Reactor Calculations. Nuclear and Radiological Engineering/Medical Physics. Atlanta, GA, Georgia Institute of Technology. **PhD:** 142.

Forget, B. and F. Rahnema (2005). Improved Monte Carlo Adaptation of the Heterogeneous Coarse-Mesh Transport Method. The Monte Carlo Method: Versatility Unbounded In A Dynamic Computing World. Chattanooga, TN.

Foulke, L. R. and E. P. Gyftopoulos (1967). "Application of the Natural Mode Approximation to Space-Time Reactor Problems." Nuclear Science and Engineering **30**(3): 419-435.

Goluoglu, S. and H. L. Dodds (2001). "A Time-Dependent, Three-Dimensional Neutron Transport Methodology." Nuclear Science and Engineering **139**: 248-261.

Griesheimer, D., W. Martin, et al. (2005). "Estimation of Flux Distributions With Monte Carlo Functional Expansion Tallies." Radiation Protection Dosimetry **115**(1-4): 428-432.

Griesheimer, D. P., W. R. Martin, et al. (2006). "Convergence Properties of Monte Carlo Functional Expansion Tallies." Journal of Computational Physics **211**: 129-153.

Hetrick, D. L. (1971). Dynamics of Nuclear Reactors. Chicago, The University Press of Chicago.

Kaplan, S. (1961). "The Property of Finality and the Analysis of Problems in Reactor Space-Time Kinetics by Various Modal Expansions." Nuclear Science and Engineering **9**(3): 357-361.

Kaplan, S. (1966). "Synthesis Methods in Reactor Analysis." Advances in Nuclear Science Technology **3**: 233.

Kornreich, D. E. and D. K. Parsons (2005). "Time-Eigenvalue Calculations in Multi-Region Cartesian Geometry Using Green's Functions." Annals of Nuclear Energy **32**: 964-985.

Larsen, E. W. and P. F. Zweifel (1974). "On the Spectrum of the Linear Transport Operator." Journal of Mathematical Physics **15**(11): 1987-1997.

Lewis, E. E. and J. W. F. Miller (1993). Computational Methods of Neutron Transport. La Grange Park, IL, American Nuclear Society.

Linz, P. (1985). Analytical and Numerical Methods for Volterra Equations. Philadelphia, SIAM.

Montagnini, B., P. Raffaelli, et al. (1996). "A 3D Coarse-Mesh Time Dependent Code for Nuclear Reactor Kinetic Calculations." Annals of Nuclear Energy **23**(6): 517-532.

Mosher, S. and F. Rahnema (2006). "The Incident Flux Response Expansion Method for Heterogeneous Coarse Mesh Transport Problems." Transport Theory and Statistical Physics **35**(1): 55-86.

Olson, K. R. and D. L. Henderson (2004). "Numerical Benchmark Solutions For Time-Dependent Neutral Particle Transport In One-Dimensional Homogeneous Media Using Integral Transport." Annals of Nuclear Energy **31**: 1495-1537.

Ott, K. O. and D. A. Meneley (1969). "Accuracy of the Quasistatic Treatment of Spatial Reactor Kinetics." Nuclear Science and Engineering **36**(3): 402-411.

Pautz, A. and A. Birkhofer (2003). "DORT-TD: A Transient Neutron Transport Code with Fully Implicit Time Integration." Nuclear Science and Engineering **145**: 299-319.

Richtmyer, R. D. (1957). Difference Methods for Initial Value Problems. New York, Interscience Publishers, Inc.

Smith, K. S. (1986). "Assembly Homogenization Techniques For Light Water Reactor Analysis." Progress in Nuclear Energy **17**(3): 303-335.

Spanier, J. (1999). "Monte Carlo Methods for Flux Expansion Solutions of Transport Problems." Nuclear Science and Engineering **133**: 73-79.

Stacey, W. (2001). Nuclear Reactor Physics. New York, John Wiley & Sons, Inc.

Stamm'ler, R. J. J. and M. J. Abbate (1983). Methods of Steady-State Reactor Physics in Nuclear Design. London, Academic Press.

Sutton, T. M. and B. N. Aviles (1996). "Diffusion Theory Methods for Spatial Kinetics Calculations." Progress in Nuclear Energy **30**(2): 119-182.

Turinsky, P. (2001). NESTLE v5.2.0: Few-Group Diffusion Equation Solver Utilizing the Nodal Expansion Method for Eigenvalue, Adjoint, Fixed-Source Steady-State and Transient Problems, Electric Power Research Center, North Carolina State University.

VITA

Justin Michael Pounders was born on March 4, 1983, in Mobile, Alabama, to Dr. Randy and Lynda Pounders. He spent the first 13 years of his life growing up in northwest Alabama with his brother, Jason, and sister, Emily. In 1997, he moved with his family to southern China. He lived for seven months in Nanning, Guangxi, before moving to Kunming, Yunnan, for four years where he was also blessed with another sister, Anna Grace. He graduated from the Kunming International Academy in 2001 and began undergraduate studies in nuclear engineering the following fall at the Georgia Institute of Technology in Atlanta. He received a Bachelor of Science from Georgia Tech in 2005 and a Master of Science in 2006 with the thesis, "Stochastically Generated Multigroup Diffusion Coefficients." In 2005, he was appointed to the Rickover Graduate Fellowship program (formerly the Naval Nuclear Propulsion fellowship program) that supported him throughout his graduate studies and through which he spent two summers working at Bettis Atomic Power Laboratory in Pittsburgh, PA. He has been married to his wife, Sarah, since May 2005.